

EXTERNAL MEMORANDUM NO. 21

PROJECT MX-794

(AAF Contract W33-038 ac 14222)

MEASUREMENT OF FLAME SPEEDS WITH THE V-FLAME

By

R. B. MORRISON

R. A. DUNLAP

May 1948

PREFACE

This is a termination report covering a phase of the basic propulsion research specified in AAF Contract MX794. This work, which was undertaken at the University of Michigan in September, 1946, and which was completed in May, 1948, is partially reported in Progress Reports covering the work under the subject contract. The authors would like to acknowledge the assistance given by Professor A. S. Foust, Dr. D. T. Williams, and Messrs. T. Barnes, W. L. Culligan, and I. L. Hanson.

TABLE OF CONTENTS

Preface	i
List of Figures	iii
List of Symbols	v
Introduction	1
Results	2
Summary of Bunsen Burner Methods of Measuring Flame Speeds	3
Analysis of the V-Flame	
1. An Area Analysis of the V-Flame	6
2. A Modified Huygen's Wave Analysis of the V-Flame	8
3. A Steady Flow Analysis of the V-Flame	11
Discussion	
1. A Comparison of the Bunsen Burner Methods	13
2. Discussion of the V-Flame Method of Flame Speed Measurement	13
Appendix	
1. Measurement of Bunsen Flame Speeds	21
2. Measurement of V-Flame Speeds	23
3. Method of Taking Shadowgraphs	30
References	31
List of Illustrations	32

LIST OF FIGURES

<u>FIGURE NO.</u>	<u>TITLE</u>	<u>PAGE</u>
1	Stationary Flame in a Closed Tube	4
2	Typical Bunsen Burner Flame	4
3	Streamline Flow Pattern about a Conical V-Flame	7
4	Discontinuity Formed by a Disturbance	8
5	Flame in a Constant Area Duct	10
6	Vector diagram of Velocities at Flame Front	12
7	Comparison of Area and Angle Methods of Measuring Bunsen Flame Speeds	14
8	Flame Speeds for Propane Flame as Measured by Different Methods	15
9	Pressure Integral around V-Flame	17
10	Graph of Flame Angle vs. Power in Watts and Temperature	18
11	Graph Showing variation in Flame Angle using Different Size Flame Holders	18
12	Bunsen Burner Test System	21
13	Effect of Water Vapor on Flame Speed	22
14	Total Pressure Traverse Across Nozzle Exit	24
15	The V-Flame System for Measuring Flame Speeds	25
16	Theroetical Flame Temperatures of a Propane- Air Flame	26
17	Density Ratio Across Flame Front	27

LIST OF FIGURES

<u>FIGURE NO.</u>	<u>TITLE</u>	<u>PAGE</u>
1	Stationary Flame in a Closed Tube	4
2	Typical Bunsen Burner Flame	4
3	Streamline Flow Pattern about a Conical V-Flame	7
4	Discontinuity Formed by a Disturbance	8
5	Flame in a Constant Area Duct	10
6	Vector diagram of Velocities at Flame Front	12
7	Comparison of Area and Angle Methods of Measuring Bunsen Flame Speeds	14
8	Flame Speeds for Propane Flame as Measured by Different Methods	15
9	Pressure Integral around V-Flame	17
10	Graph of Flame Angle vs. Power in Watts and Temperature	18
11	Graph Showing variation in Flame Angle using Different Size Flame Holders	18
12	Bunsen Burner Test System	21
13	Effect of Water Vapor on Flame Speed	22
14	Total Pressure Traverse Across Nozzle Exit	24
15	The V-Flame System for Measuring Flame Speeds	25
16	Theroetical Flame Temperatures of a Propane- Air Flame	26
17	Density Ratio Across Flame Front	27

LIST OF FIGURES

<u>FIGURE NO.</u>	<u>TITLE</u>	<u>PAGE</u>
18	Streamlines Used for the V-Flame Area Method of Measuring Flame Speeds	29
19	Shadowgraph System	30

S Y M B O L S

A_a	- Area of circle where a is the diameter
A_f	- Surface area of revolution of flame surface
A_j	- Cross sectional area of jet
P_B	- Barometric pressure
P_b	- Pressure of the burned charge just after leaving flame
P_j	- Pressure of issuing jet of gas mixture
P_u	- Pressure of the unburned charge just prior to entering flame
Q_{air}	- Volume flow of air
Q_{prop}	- Volume flow of propane gas
Q_j	- Total volume flow issuing from jet
R	- Gas constant
R_b	- Radius of Bunsen Burner
T_b	- Temperature of burned gases
T_u	- Temperature of unburned gases
V_b	- Velocity of the burned charge just after leaving flame
V_{bn}	- Component of V_b normal to flame surface
V_{bt}	- Component of V_b parallel to flame surface
V_e	- Velocity after burning in a duct
V_f	- Flame speed as defined on Page 1
V_j	- Velocity of issuing jet
V_s	- Spatial velocity of a disturbance wave
V_u	- Velocity of the unburned charge just prior to entering flame
V_{un}	- Component of V_u normal to flame surface
V_{ut}	- Component of V_u parallel to flame surface
a	- Distance between streamlines issuing from jet
b	- Distance between streamlines at flame surface
d	- Diameter of flame holder
e	- Vapor pressure of water vapor
r	- Radius of combustion sphere
α	- Angle between streamline and flame surface before burning
v	- Specific volume

S Y M B O L S

(continued)

- β - Angle between streamline and flame surface
after burning
- δ - Diameter of button flame holder
- θ - Angle between flame surfaces
- ρ_b - Density of burned gases
- ρ_u - Density of unburned gases
- F/A - Wgt. fuel/wgt. of dry air

INTRODUCTION

One problem associated with combustion is the speed at which a flame front traverses a combustible mixture. In the past such knowledge of "flame speed"* served as a means to characterize fuels which were used in internal combustion engines, furnaces, torches, etc. In the field of jet propulsion, an even greater significance is attached to the subject because the combustion chamber characteristics of jet devices are intimately connected with the flame speed of the fuel used. Practical experience indicates that blow-off, incomplete combustion, and combustion instabilities are frequent when the velocities of the unburned mixture exceed 200 to 250 ft/sec. Various methods have been suggested to remedy the above undesirable situations, such as flame holder design, introduction of turbulence, new fuels, and combustion chamber design. Any or all of the latter could well influence the propagation speeds of the flame. Such procedures as the Bunsen burner method (Ref.1) and the soap bubble method (Ref.2) of measuring flame speed do not readily lend themselves to the study of flame speeds under the above imposed conditions. For example, it seems unlikely that the soap bubble method could be used to study the effect of turbulence on flame speed. Also, in the case of the Bunsen burner method it is necessary to observe the flame surface through burned or burning mixtures which eliminates the use of fuels with opaque products of combustion. These methods also offer difficulties in the case of flame propagation through fuel mists. Therefore, the measurement of flame speeds with the V-flame, which has received little attention in the past and which possesses some inherent advantages over the above mentioned methods, was investigated.

*Flame speed is defined in this report as the rate at which a flame front traverses a stagnant combustible mixture relative to the unburned gas in a direction normal to the flame surface. The flame speeds defined in this manner should not be confused with flame speeds defined relative to a fixed point in space or relative to the burned gases.

RESULTS

The V-flame phenomenon provides a suitable datum for flame speed measurement which is particularly adaptable to the study of flames with turbulence, to propagation of flames in fuel mists or to flames which have opaque products of combustion. The datum was verified by a V-flame area method which closely checked the Bunsen area method. A simple theory for using the datum is given by $V_f = \rho_b / \rho_u V_j \sin \theta / 2$ for which the variables can be readily determined. Discrepancies in this method and various other methods of flame speed measurement are discussed.

Use was made of talc particles and titanium tetrachloride smoke streams to describe the flow pattern in advance and behind the flame front. While the method using talc particles was adequate, the method utilizing titanium tetrachloride provided a single streamline of high contrast from which quantitative data could easily be taken.

A BRIEF SUMMARY OF THE BUNSEN BURNER METHOD
OF MEASURING FLAME SPEED

One of the first attempts to measure flame speed was made by Bunsen in the middle of the nineteenth century. (Ref.3) He considered, as shown in Figure 1, a stationary flame front in a tube of flowing combustible gas. If the velocity, V_u , of the unburned gas is adjusted so that the flame front is stationary relative to the tube wall, then the velocity, V_u , is, by definition, equal to the flame speed.

However, since it is difficult to eliminate the boundary layer region of low velocity in the vicinity of the tube wall, a stationary flame front is hard to maintain. This practical difficulty makes the latter method unsuitable for quantitative measurement.

Another means commonly employed for measuring flame speed is the Bunsen burner method. This method which was first proposed by Guoy and later refined by others (Ref. 1) is briefly given here.

Consider the Bunsen burner flame surfaces shown in Figure 2. By conservation of mass flow across the flame surface:

$$\rho_u \bar{V}_j A_j = \rho_u V_f A_f$$

or

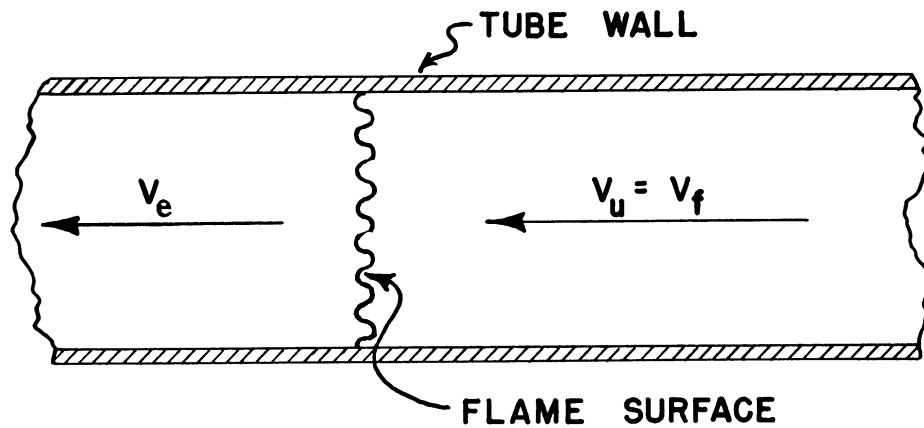
$$V_f = \bar{V}_j \frac{A_j}{A_f} = \frac{Q_j}{A_f} \quad (1)$$

where \bar{V}_j is the average jet velocity.

If the velocity is assumed to be constant over the entire cross section of the tube, then the flame surface is, as shown in Figure 2a, a true cone and

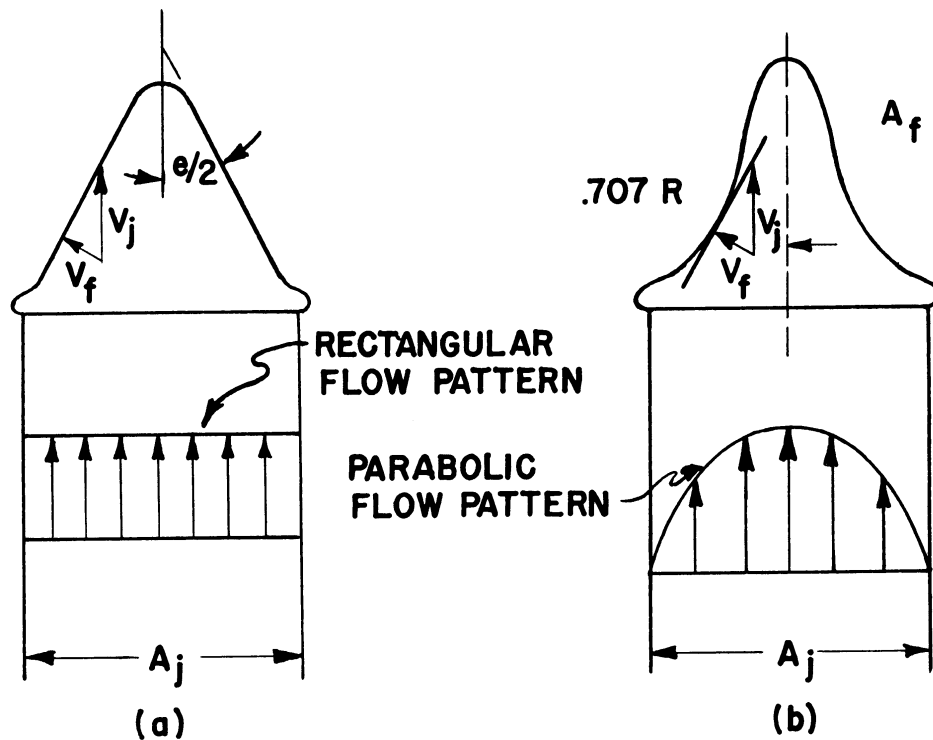
$$V_f = \bar{V}_j \sin \theta / 2$$

If the velocity distribution of the issuing jet of gas is parabolic (Figure 2b), the velocity measured at .707 R is equal to \bar{V}_j or



STATIONARY FLAME IN A CLOSED TUBE

FIGURE 1



TYPICAL BUNSEN BURNER FLAME

FIGURE 2

$$V_f = \bar{V}_j \sin \theta / 2_{at} .707 R \quad (2)$$

The method defined by equation (1) i.e., the Bunsen area method, was that used by Guoy in his work on flame propagation. Smith and Pickering (Ref. 4) used the method defined by equation (2), i.e., the Bunsen angle method, as an expedient means of determining flame speeds for their work on flame propagation.

Both the Bunsen area and Bunsen angle method for measuring flame speeds were used in certain phases of the work covered in this report. The results of the two methods do not completely agree with each other as is shown in Figure 7. The Bunsen area method is based on the assumption that the flame speed is constant over the entire flame surface while the Bunsen angle method assumes that the laminar parabolic velocity distribution in the tube remains unchanged outside the tube. It is felt that the Bunsen area method, which had less experimental error and which is based on safer assumptions than the Bunsen angle method, is superior to the Bunsen angle method for measuring flame speeds. Therefore, flame speeds found by the Bunsen area method are used in all cases where Bunsen flame speeds are called for.

ANALYSIS OF THE V-FLAME

The V-flame phenomenon (See illustration 2, page 34) can be observed if an obstruction of sufficient size is held in a moving stream of combustible gas and the gas then ignited in the immediate vicinity of the obstruction. The obstruction or "flame holder" creates a zone of sufficiently low velocity in its wake that combustion can take place there, and hence, this region serves as an ignition source to the moving stream. The flame propagates outward from the flame holder giving the characteristic V appearance.

The brush around the top of the flame occurs as a consequence of the gas jet mixing with the surrounding stationary air. The brush is of no consequence in the case of lean mixtures where the mixing produces still leaner mixtures and therefore very slow burning flames. In such cases the brush almost disappears as can be seen in Illust.3, p. 35. With rich mixtures the mixing produces a faster burning flame which tries to travel down the mixing region to the rim of the nozzle. If the jet velocity is sufficiently high, the latter is impossible, but the burning in the eddies of this mixing zone produces considerable fluctuation of the brush.

1) An Area Analysis of the V-Flame

Consider as in Figure 3 a conical V flame with its apex at O. Further, let x-x represent streamlines intersecting the flame surface at A. (Illust. 1, p. 33 for a photograph of the V-flame with streamlines introduced by smoke probes.) Conservation of mass requires that the mass flow across "a" equal the mass flow across the surface of revolution generated by the line OA.

Since the rate at which the unburned gas moves normal to the surface OA is flame speed:

$$\rho_u A_f V_f = \rho_u A_a V_j$$

or

$$V_f = A_a / A_f \times V_j$$

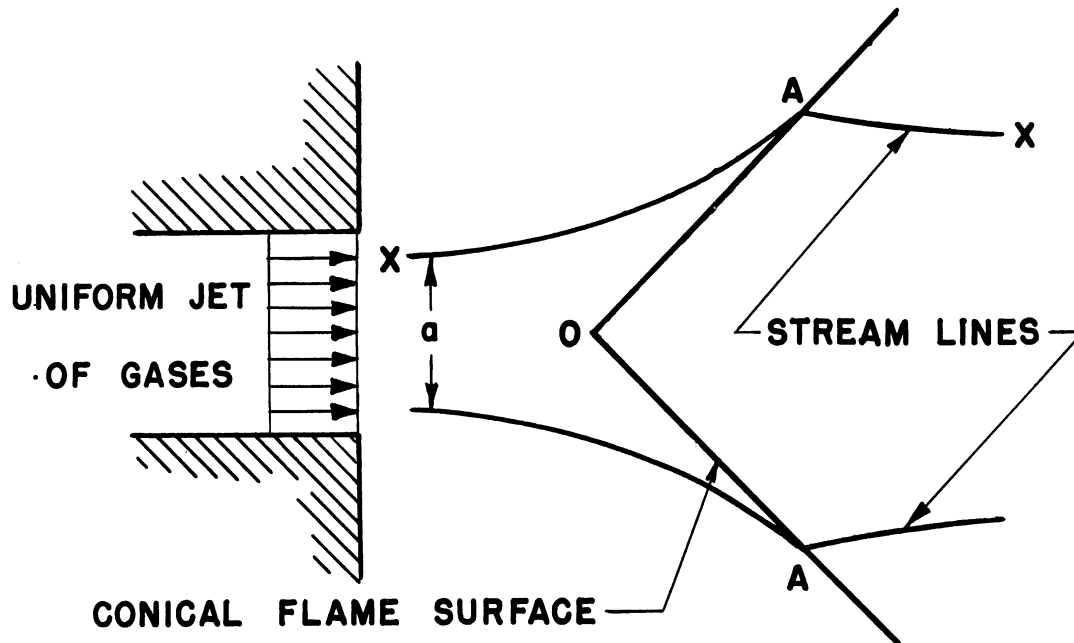


FIGURE 3
STREAMLINE FLOW PATTERN ABOUT
A CONICAL V-FLAME

where in the case of a conical flame

$$A_a = \frac{\pi}{4} a^2$$

A_f = Surface area of revolution of OA

V_j = Jet velocity

Flame speeds obtained in such a manner define an average flame speed between points O and A on the flame surface. Curve B in Figure 8 is an example of flame speeds computed by this method. The data necessary to obtain flame speeds in this manner requires the use of smoke or some such means to indicate the position of the streamlines. It was found difficult to produce smoke streamers for reasons which are discussed in the Appendix.

2. A Modified Huygen's Wave Analysis of the V-Flame

The flame front of the V-flame might be considered as the type of discontinuity which results from a series of disturbances moving at constant velocity through a stagnant gas. As the number of these disturbance centers is increased to infinity, the surface of discontinuity develops as a cone shown in Figure 4 with the axis along ON and the vertex at O, which results in:

$$V_s = V_j \sin \theta/2$$

where V_s is the rate of

propagation of the disturbance. If there were no change in specific volume across the disturbance front, i.e., no expansion behind the front, then V_s in the case of combustion would be V_f , the normal flame speed relative to the ignition centers.

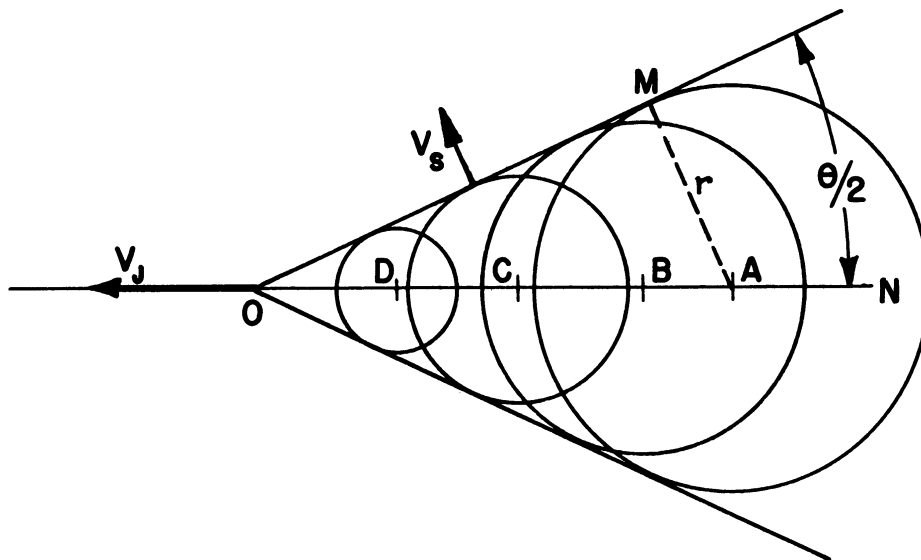


FIGURE 4

DISCONTINUITY FORMED BY A DISTURBANCE

In combustion, however, there is an increase in the specific volume from one side to the other side of the disturbance front which is now referred to as the flame front. A correction for this expansion can be applied to the above Huygen's wave approach if the disturbance centers, now called ignition centers (A,B,C,D,etc.), remain stationary as the combustion proceeds. This assumption will lead to a discrepancy from the actual flame speeds for reasons discussed later in this report.

For this correction, due to change in specific volume, consider a burning sphere of radius r at time t . The rate at which the gas is burned is $V_f 4\pi r^2$, so in time dt the volume of the charge burned is $V_f 4\pi r^2 dt$. This volume, however, is expanded due to the density decrease across the burning zone and so the actual increase of the volume $V_f 4\pi r^2 dt$ when burned is

$$\frac{\rho_u}{\rho_b} 4\pi r^2 V_f dt$$

where ρ_u and ρ_b refer to the density before and after combustion respectively.

Also:

dv = differential volume of combustion sphere

$$= 4\pi r^2 dr$$

$$\text{then } 4\pi r^2 dr = 4\pi r^2 \frac{\rho_u}{\rho_b} V_f dt$$

$$\text{or } \frac{dr}{dt} \frac{\rho_b}{\rho_u} = V_f$$

Now $\frac{dr}{dt} = V_s$ = the velocity with which the flame surface moves relative to point O (Figure 4), i.e., the actual spatial velocity of the flame. In the case of an ignition point moving at velocity V_j then from Figure 4

$$V_s = V_j \sin \theta / 2$$

but

$$V_s = V_f \frac{\rho_u}{\rho_b}$$

$$\text{so } V_f = V_j \frac{\rho_b}{\rho_u} \sin \theta/2 \quad (4)$$

An alternate expression for (4) follows if the burning process is regarded as a heat addition to an air cycle. Let P_u , ρ_u , and T_u be conditions before the front and P_b , ρ_b , and T_b be conditions behind the front.

$$\left. \begin{array}{l} \text{Then } P_u = \rho_u R T_u \\ \text{and } P_b = \rho_b R T_b \end{array} \right\} \text{Equation of State} \quad (5)$$

The pressure change across a flame front where the propagation velocity is low is very small as may be seen from the following analysis of a flame surface in a moving stream as shown in Figure 5.

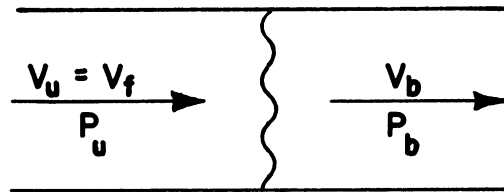


FIGURE 5

FLAME IN A CONSTANT AREA DUCT

$$\rho_u V_f = \rho_b V_b \quad \text{Conservation of mass}$$

and

$$P_u + \rho_u V_f^2 = P_b + \rho_b V_b^2 \quad \text{Momentum equation}$$

or

$$P_u - P_b = \rho_b V_b^2 - \rho_u V_f^2$$

and by combining the above two equations, we get:

$$P_u - P_b = \rho_u V_f^2 \left[\frac{\rho_u}{\rho_b} - 1 \right]$$

The maximum observed values of V_f and $\frac{\rho_u}{\rho_b}$ are not in excess of

1.5 feet/second and 5 respectively for a propane flame. The maximum pressure difference across this flame is then in the order of

$$\begin{aligned} P_u - P_b &= .002378 \times 2.25 \times 5 \\ &= .0268 \text{ lb/ft}^2 \text{ or } .00001265 \text{ atm.} \end{aligned}$$

Since $P_b \approx P_u$, then from (5)

$$\frac{\rho_b}{\rho_u} = \frac{T_u}{T_b}$$

or equation (4) becomes:

$$V_f = V_j \frac{T_u}{T_b} \sin \theta / 2 \quad (6)$$

for a heat addition to an air cycle.

3. A Steady Flow Analysis of the V-Flame

A steady flow analysis of the V-flame yields essentially the same expression for flame speed and gives some additional information concerning the flow pattern. Consider as in Figure 6 the flame front OA where V_u is the velocity of the unburned gas, V_b the velocity of the burned gas and where the subscripts n and t denote a direction perpendicular and parallel to the front respectively. Assuming no momentum exchange parallel to the front, a momentum balance taken along the front is then:

$$\rho_u V_{un} V_{ut} = \rho_b V_{bt} V_{bn}. \quad (7a)$$

From conservation of mass

$$\rho_u V_{un} = \rho_b V_{bn} \text{ it follows that } V_{ut} = V_{bt}$$

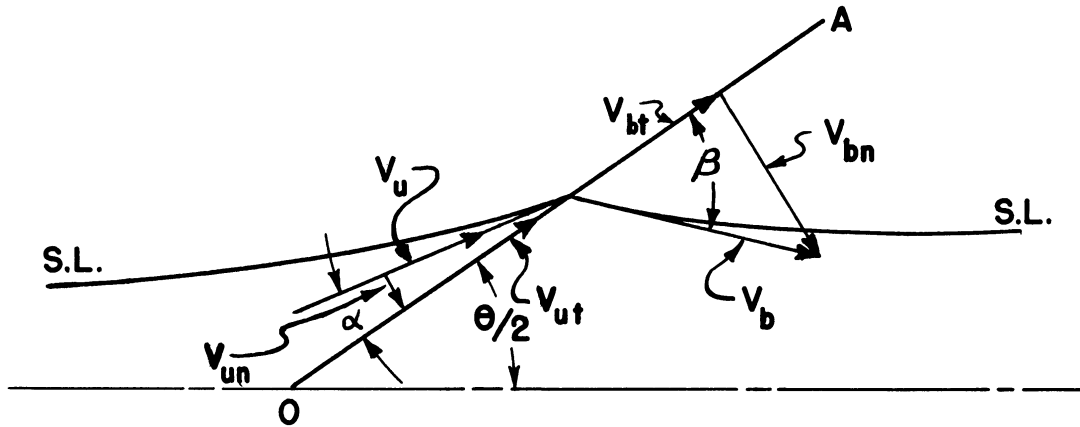


FIGURE 6

Equation 7a may now be written as:

$$\frac{\rho_b}{\rho_u} = \frac{V_{un}}{V_{bn}} = \frac{\tan \alpha}{\tan \beta} \quad (7b)$$

This relation was used in the experimental determination of ρ_b / ρ_u

Since V_{un} is the rate at which the flame surface enters the unburned charge, it is V_f and

$$V_f = V_u \sin \alpha$$

or putting V_f in terms of V_b and β :

$$V_f = \rho_b / \rho_u V_b \sin \beta = \rho_b / \rho_u V_{bn} \quad (8)$$

If $V_b = V_j$ and $\theta / 2 = \beta$, i.e., if the flow after burning were parallel to the axis of the flame, the original equation

$$V_f = V_j \rho_b / \rho_u \sin \theta / 2 \quad (4)$$

would result from Equation 8. However, as is discussed later in the report, β was observed to be larger than $\theta / 2$ and V_b probably is not equal to V_j .

DISCUSSION

Four of the methods previously discussed, i.e., Bunsen burner angle and area method and the V-flame angle and area method, were used for measuring flame speeds. Figure 7 shows a comparison between flame speeds as computed by the Bunsen burner area method and the Bunsen burner angle method as is derived on page 3. Figure 8 shows flame speed measured by the Bunsen burner area method as compared to flame speed measured by the V-flame angle method and the V-flame area method.

1. A Comparison of the Bunsen Burner Methods

As is shown in Figure 7 the flame speeds computed by the two Bunsen burner methods do not completely agree with each other. There are a number of explanations which might predict these discrepancies. For example, if the flame speed is not constant over the entire flame surface, the area method which measures an average flame speed will not agree with the angle method which measures flame speed at a point on the flame surface. Another reason might possibly be that the airflow, while having a parabolic distribution in the burner tube,* does not have a parabolic distribution at the flame surface. If this is the case, the V_j measured at .707 R is not the average V_j so that the equation

$$V_f = V_j \sin \theta / 2 \quad .707 R$$

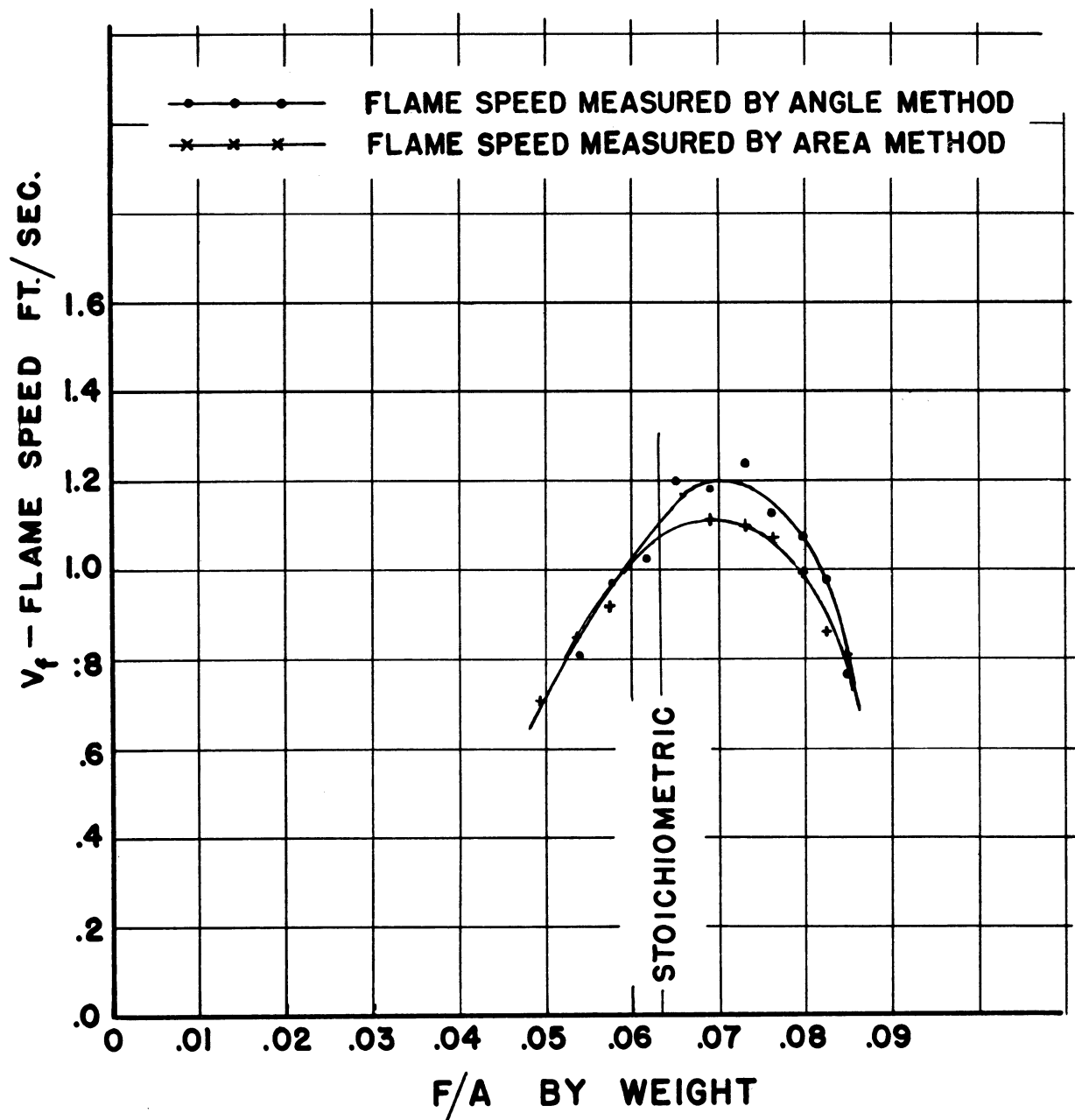
does not hold. Since the area method measures an average flame speed and gives the most consistent results, it is used in the comparison with the V-flame methods.

2. Discussion of the V-flame Method of Flame Speed Measurement

Figure 8 illustrates the results obtained from the V-flame and Bunsen methods of flame speed measurement for propane-air mixtures. Since the data for the Bunsen and V-flame were taken as simultaneously as possible from a common source of gas-air mixture, the F/A ratio and the humidity of both the Bunsen burner flame and the V-flame were identical. Therefore, any discrepancies of the three curves from one another can be attributed either to V_f being a function of the physical system, to some error in the theory, or to some consistent error in the measurement of the physical geometry of the flame.

* See page 21.

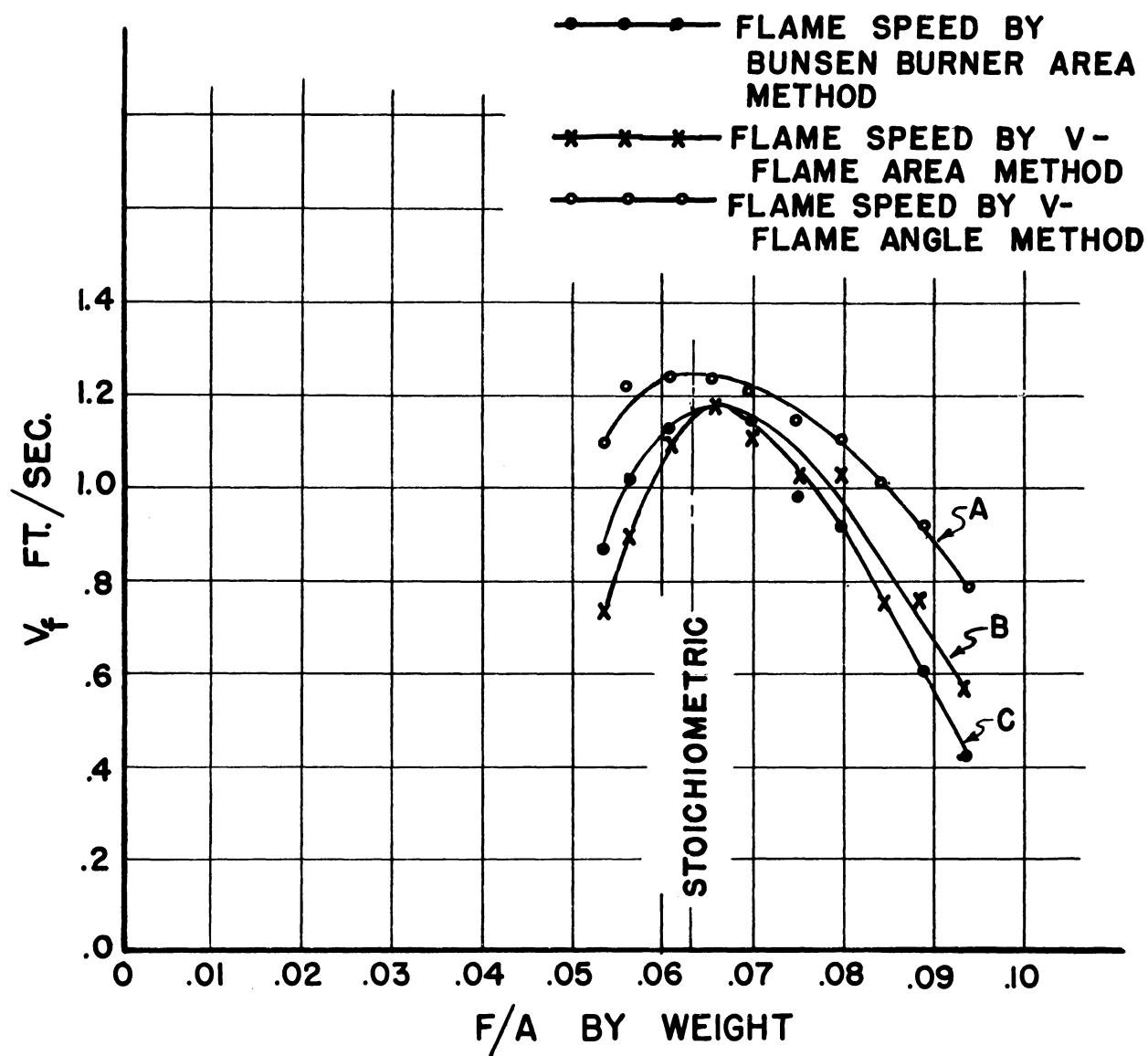
UMM-21



COMPARISON OF AREA AND ANGLE METHODS OF MEASURING BUNSEN FLAME SPEEDS FOR A PROPANE FLAME UNSATURATED MOISTURE CONDITION.

FIGURE 7

UMM-21



FLAME SPEEDS FOR PROPANE FLAME AS
MEASURED BY DIFFERENT METHODS.

FIGURE 8

The density ratios used in Equation 4 for the calculations of curve A (Figure 8) were obtained from a graph of experimental values of ρ_b / ρ_u . This graph was determined by the variables, α and β in equation

$$\frac{\rho_b}{\rho_u} = \frac{\tan \alpha}{\tan \beta} \quad (7b)$$

which was derived from momentum and mass considerations across a flame front. To establish α (which was always a small angle, in the order of a few degrees) it was necessary to track the smoke trace of a streamline for a short distance in advance of the flame front. Because the streamline is curved (illust.1, p.33), the tendency might be to measure the angle α larger than the true value at the flame front. The angle β , which was large, gives a small percentagewise error.

Since $V_f = V_j \rho_b / \rho_u \sin \theta / 2$ is the equation used to plot curve A, any error incurred in measuring α larger than the actual value of α at the front would result, in light of equation 4, in the computed V_f being too large.

The curves A and B in Figure 8 are not only displaced vertically but have a difference in shape. The difference in shape, however, cannot be attributed to an error in the measurement of ρ_b / ρ_u , ρ_b / ρ_u being a nearly constant multiplier. For this reason it is felt that this discrepancy is due to an error in the theory used to compute these flame speeds.

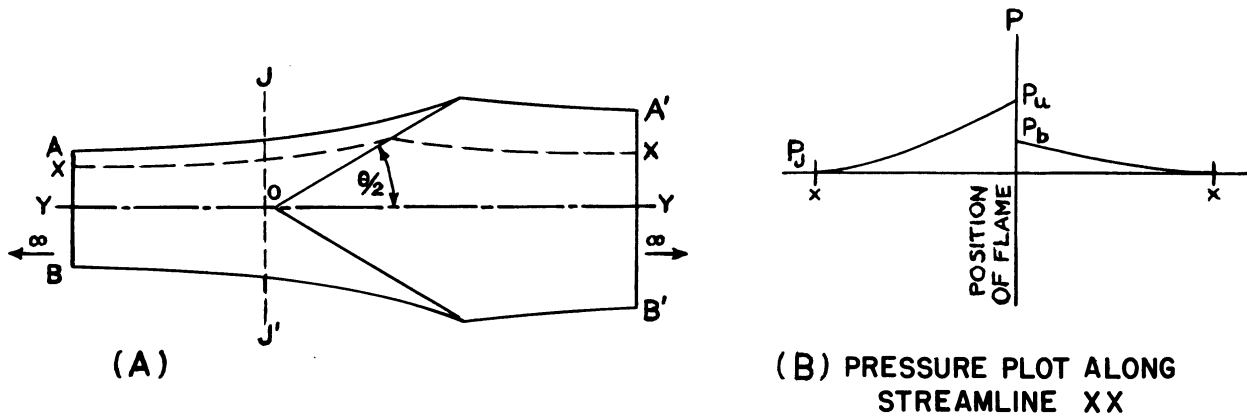
The analysis appearing on page 8 which yields

$$V_f = V_j \rho_b / \rho_u \sin \theta / 2 \quad (4)$$

is based on the assumption that the velocity of an ignition center is constant along the axis of the flame (Figure 9) and that V_b is equal and parallel to V_j . These assumptions are identical with those used in the development of equation 8 of the steady flow analysis given on page 11.

The following momentum analysis of the V-flame will justify to some extent the assumption of $V_b = V_j$.

UMM-21


FIGURE 9

Take V_j to be the jet velocity at a point far in front of the flame surface where the pressure is p_b . Let A-A' and B-B' represent the boundaries of the jet of the unburned and burned mixtures. Let V_b be the velocity of the burned charge at a point sufficiently downstream of the flame that the pressure at that point is also p_b . Assume that the pressure along A-A' and B-B' to be atmospheric, an assumption which would be valid if there were no mixing of the jet with the external air and if the external system were at atmospheric pressure along A-A' and B-B'.

Consider as a system A-B-B'-A'-A. The integral of pressures around this closed path is zero, hence the momentum equation may be written as:

$$\rho_u A_{AB} V_j^2 = \rho_b A_{A'B'} V_b^2$$

if the velocities V_j and V_b across AB and A'B', respectively, are considered constant.

Conservation of mass requires that:

$$\rho_u A_{AB} V_j = \rho_b A_{A'B'} V_b$$

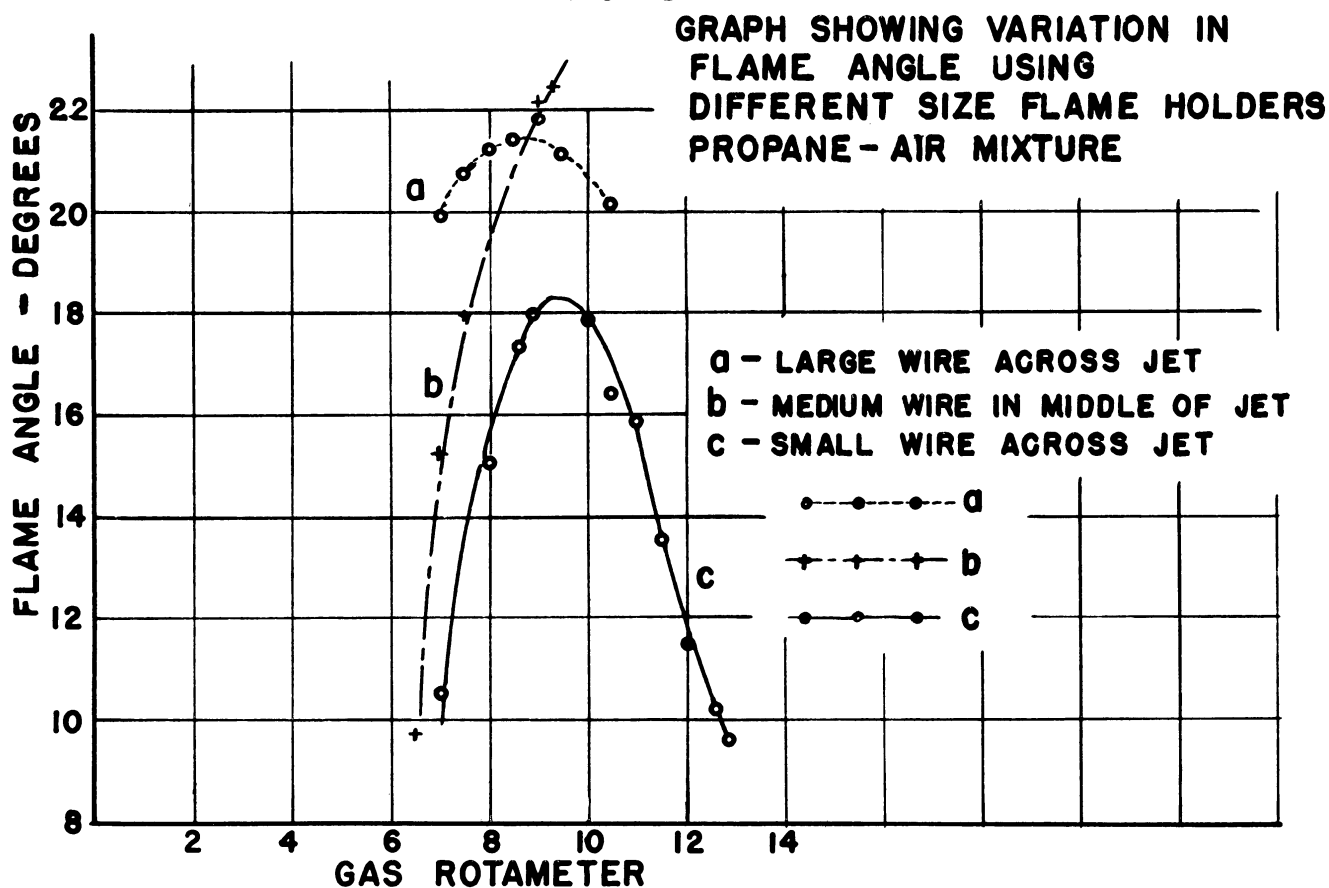
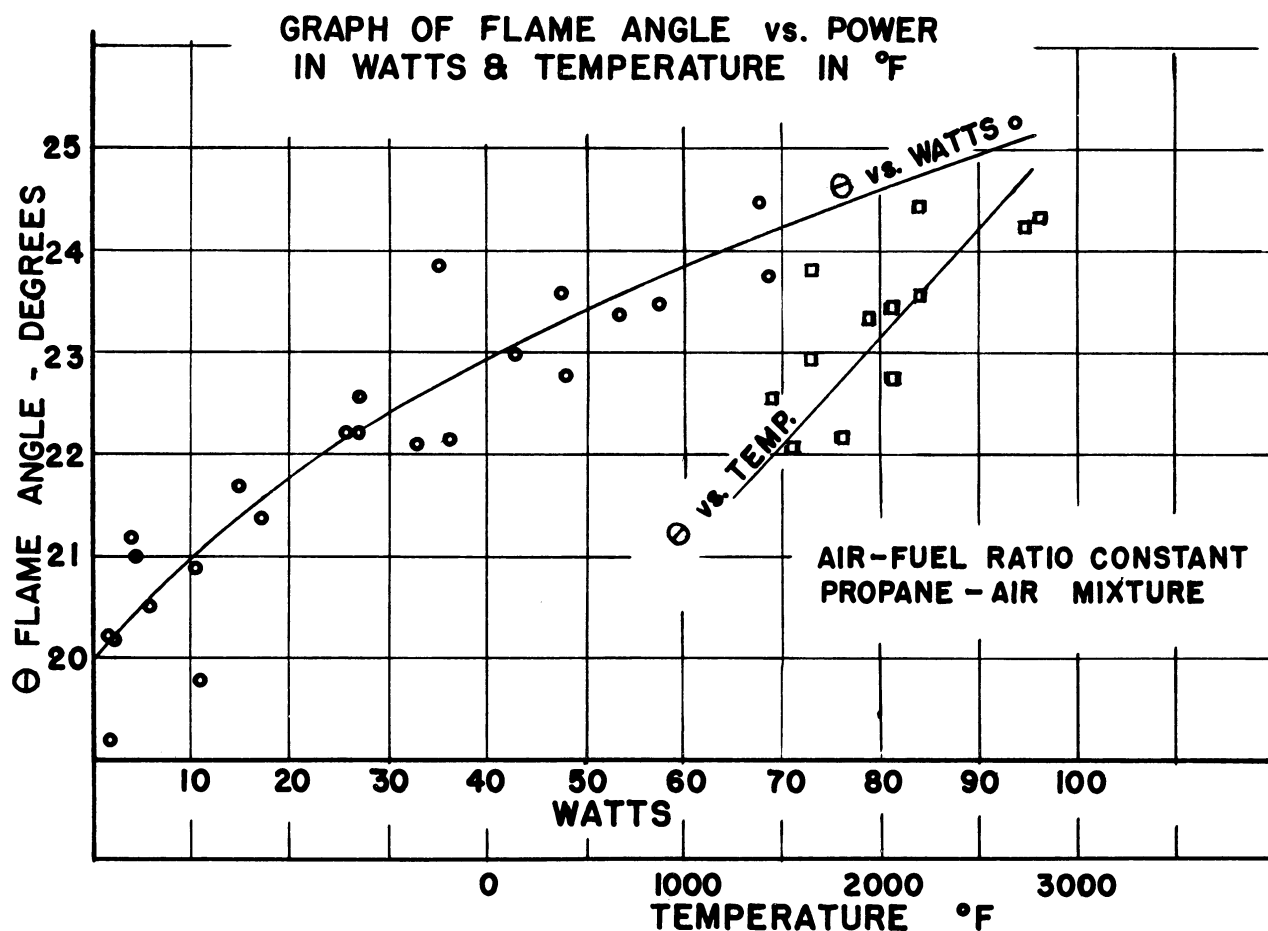
Combination of the latter two equations gives:

$$V_j = V_b$$

which substantiates the previous assumption that $V_j = V_b$.

The afore-mentioned convergence of the streamlines in the burned portion indicates that there is an acceleration of the gas after burning up to the velocity V_b . The pressure drop across the front and the pressure drop due to post flame front acceleration must be balanced by a pressure rise from a

UMM-21



diffusion process in the unburned charge. The velocity of an ignition center just downstream of 0 (Figure 9) would then be less than $V_j = V_b$. All observations of $\theta/2$ were made in the vicinity of the apex of the flame cone, but sufficiently remote from the flame holder to avoid its effect. Hence, it seems probable that the velocity of the ignition center in this region was less than the V_j used in the calculation of curve A (Figure 8), resulting in the calculated V_f being too large.

Theoretically, the jet velocity should be measured at a point sufficiently remote from the flame holder that the pressure of the issuing jet is at atmospheric pressure. Since the nozzle exit, JJ' in Figure 9, was in close proximity to the flame surface, the natural divergence of flow might well have been restricted and the pressure across JJ' greater than atmospheric. If this were the case, V_B would have been greater than the jet velocity, V_j , as measured at JJ', and the correction mentioned above would tend to be nullified.

The discrepancies between curves B and C of figure 8 can be attributed to V_f being a function of the system, an error in the theory used for the calculation of flame speeds, or to some consistent error in measurement. The V-flame area method, i.e., $V_f = A_j/A_f V_j$ was used to calculate the flame speeds of curve B, and the Bunsen area method was used to calculate curve C. It does not seem probable that the error is in the method, since both methods utilize the same principal of conservation of mass, a method which yields an average flame speed. It is possible that an error in the V-flame area method could be incurred in the measurement of the distances a, b, and δ (refer to Appendix p. 23). This error, however, would be random and would not explain the lateral shift in the two curves.

The only explanation left for the shift in the two curves is that flame speed is a function of the system used to hold the flame in the gas stream. There are a number of reasons for believing this to be the case. First, the shift just mentioned between the Bunsen burner flame speed (Figure 8, curve B) and the V-flame speed (Curve C, Figure 8) which cannot be explained by any other means. A second reason is the observed variation of the flame angle of the V-flame with different types of holders used. This variation is shown in Figure 11 where flame angle is plotted versus gas rotameter readings, all other conditions remaining constant. Since gas rotameter readings are proportional to the F/A ratio (for constant air flow) and flame angle proportional to flame speed, these curves are similar to a plot of V_f versus F/A ratio.

It was first thought an increase in the size of the flame holder might have caused an increase in the turbulence level behind the holder and in the flame front which might result in an increase in flame speed. A shadowgraph of the flow behind the holder was taken to obtain information about the flow in this region. (Illust. 7, p. 38) There was apparently no turbulence immediately behind the holder. To insure that turbulence would be shown, if it were present, a shadowgraph of the same holder in a turbulent air stream was taken (illust. 8, p. 38), and as shown in illusts. 7 and 8 (p. 38), a decided difference in flow pattern results from the turbulent air stream.

A shadowgraph was also taken to see if the flame holder caused turbulence in the flame front (illust. 5, p.37). Compared to the shadowgraph of the V-flame in a turbulent gas stream (illst. 6, p.37) there is again no apparent turbulence in the flame front due to the flame holder.

Since the increase in diameter of flame holder did not change the turbulence level in the flame the only explanation left for the increase in flame speed must be that the system, or in this case the manner in which the flame is held in the gas stream, has an effect on flame speed.

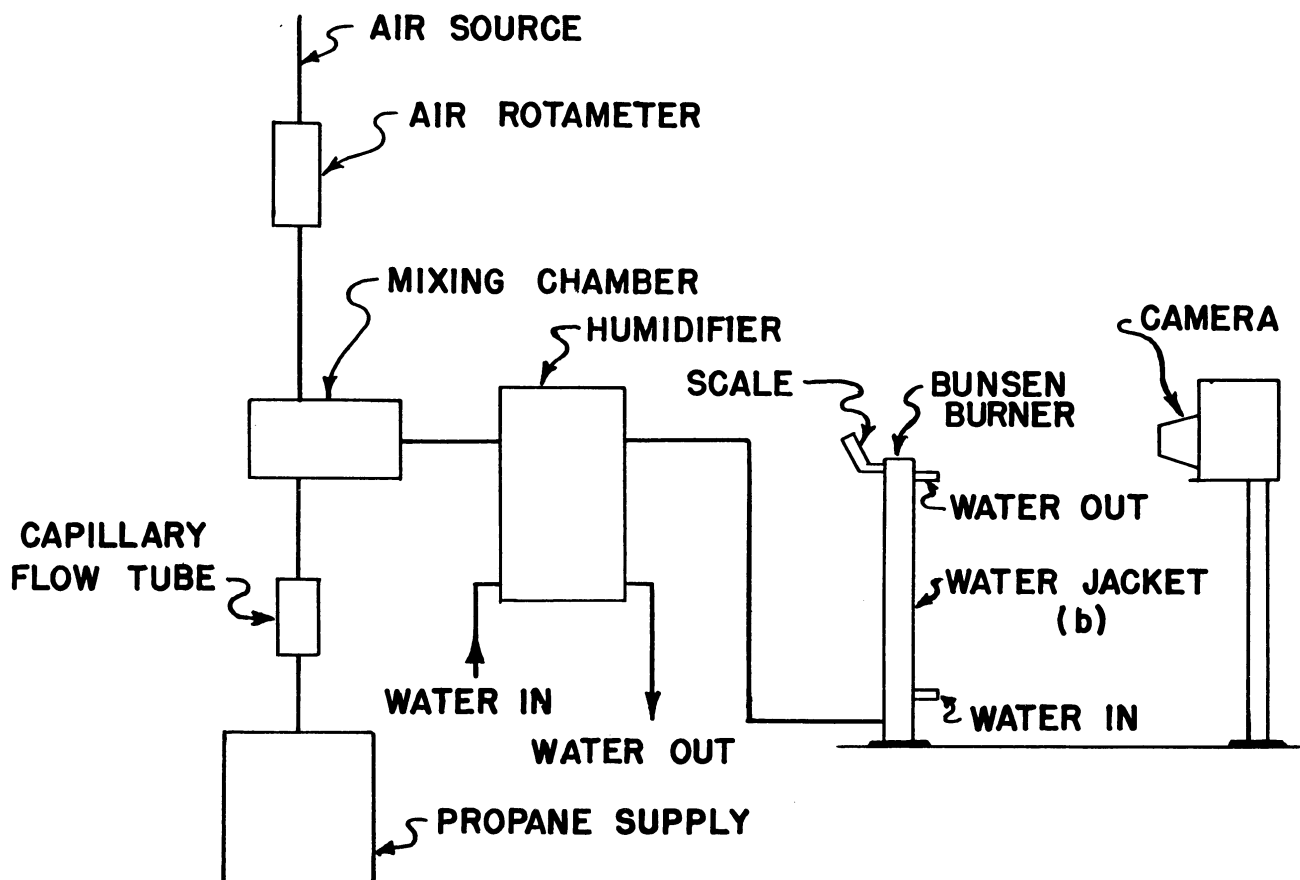
A third reason for believing flame speeds is a function of the system is the observed variation of flame angle with flame holder temperature, all other conditions remaining constant. For these runs a carbon rod flame holder was heated by passing A.C. current through it. The results are shown in Figure 10.

During the course of experiment a very interesting phenomenon was observed; namely, the existence of a pilot flame in the wake of the flame holder with the main bulk of the combustible gases passing out into the atmosphere unburned. The photograph on page 36 shows such a pilot flame. These tests were made at moderate jet speeds of 100 ft/sec and yet the flame was incapable of propagating itself laterally across the jet. This type of burning would have particular significance in a burner of a ram jet where it seems possible for most of the unburned gases to pass through the jet and never burn.

APPENDIXMEASUREMENT OF BUNSEN BURNER FLAME SPEEDS

The Bunsen burner consists of a straight tube through which a combustible mixture of air and gas flows. Refer to Figure 12 for a schematic drawing of the system used in these tests. The tube of a 75 diameter length was sufficiently long to insure that the flow in the tube was fully developed and laminar. The air flow was measured by a standard commercial rotameter. The gas flow was measured by a capillary flow tube which was calibrated by means of a positive displacement flask and a stop watch. The burner rim temperature was maintained constant throughout each run by means of the water jacket (b) around the tube.

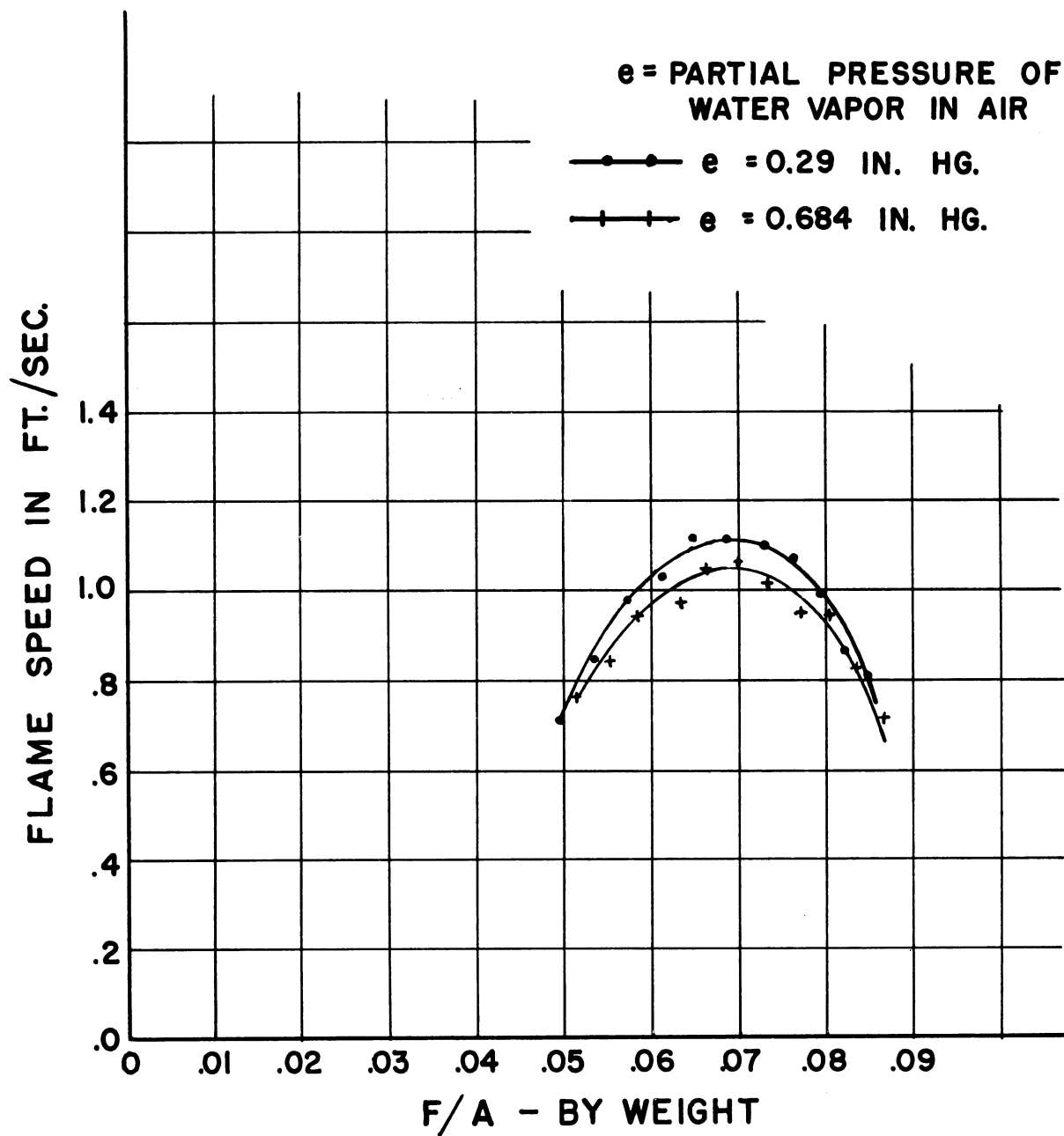
It was felt that the humidity of the air might have an effect on the flame speed and so a humidifier was placed in the system. The curves in Figure 13 show that humidity does have a decided effect on flame speed which made it necessary to keep the humidity constant throughout each run.



BUNSEN BURNER TEST SYSTEM

FIGURE 12

UMM-21



EFFECT OF WATER VAPOR ON FLAME SPEED OF
PROPANE-AIR MIXTURES. FLAME SPEEDS ARE
COMPUTED BY AREA METHOD.

FIGURE 13

The Bunsen burner flame speed was first computed by the equation

$$V_f = \frac{A_f}{A_j} V_j = A_f Q_j$$

The Q_j was the sum of the Q_{propane} and Q_{air} measured by the capillary flow tube and rotameter respectively. The area of the flame surface A_f was obtained by enlarging a photograph of the flame onto a drawing board. A Speed Graphlex camera with a red filter and a one-second exposure time was used to photograph the flame. The red filter was used so that the flame surface was distinct and so that the scale was visible. The camera was checked for any distortion by photographing a grid of parallel lines and enlarging them; the distortion of the lines was found to be negligible. The photograph was enlarged to approximately 25 times its original size and then traced onto paper. The flame surface was then considered to be a series of truncated cones, the total flame surface being the sum of the surface areas of all the truncated cones.

The other method used for computing Bunsen flame speeds was that of Smith and Pickering who used:

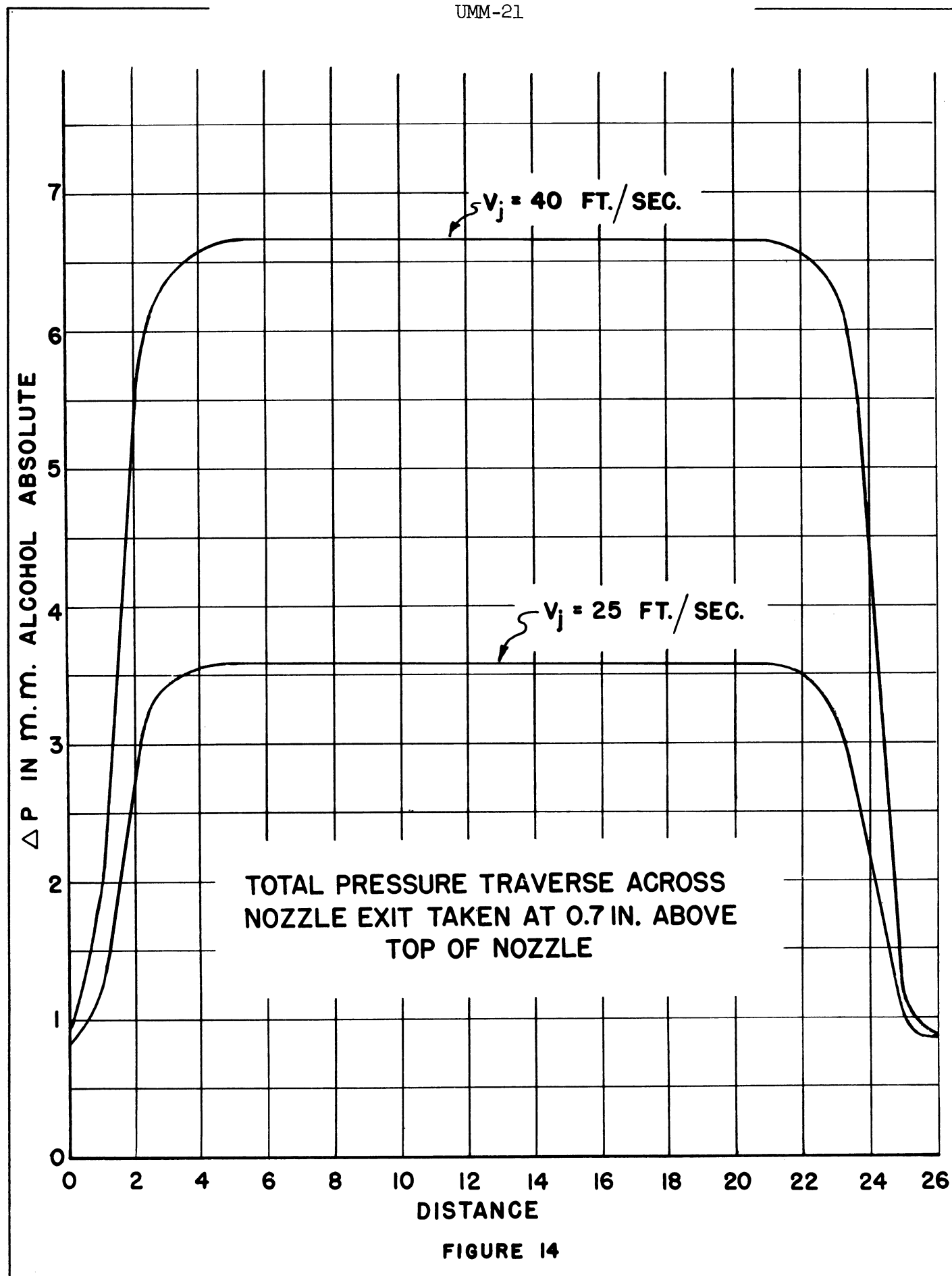
$$V_f = V_j \sin \theta/2 \quad \text{where } \theta/2 \text{ is measured at } .707 R$$

Here V_j was found by measuring the total volume flow Q which equals $Q_{\text{propane}} + Q_{\text{air}}$ and dividing this volumetric sum by the area of the jet, or $V_j = Q_j/A_j$. The photograph of the flame was enlarged as before and the angle $\theta/2$ measured from this enlargement

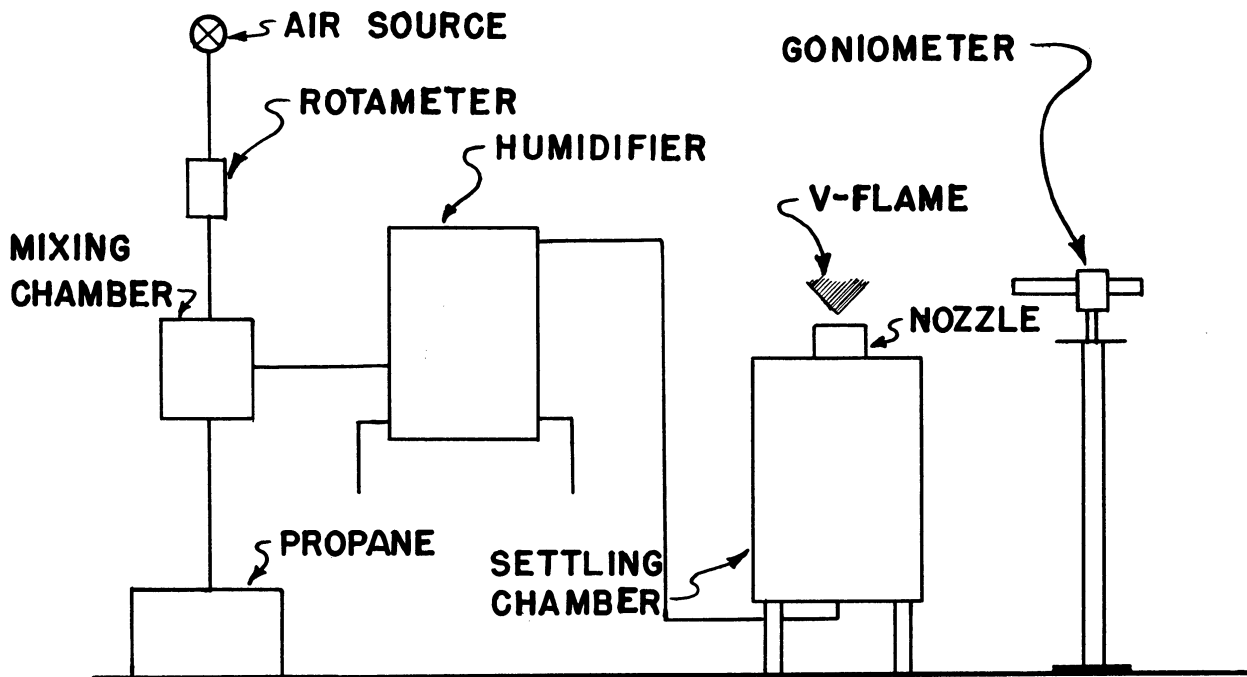
MEASUREMENT OF V-FLAME FLAME SPEEDS

The V-Flame system consisted of an air and gas supply, air and gas rotameters, the humidifier mentioned previously, a surge tank, nozzle and flame holder. A schematic diagram of this system is shown in Figure 15. The nozzle used was so designed that a nearly rectangular flow distribution of gas and air mixture issued from the jet. This distribution was checked by measuring the total head of the jet by making a micromanometer traverse of it. The results shown in Figure 14 were found to be satisfactory. Three types of flame holders were used during the course of the experiments. The first type was a small button approximately 1/16" in diameter which was suspended in the middle of the jet on a fine wire, the wire being fine enough so that it would not hold a flame. This type of holder gives a conical flame surface such as shown in the photograph, page 33. Another type of

UMM-21



holder used was a rod about $1/32$ inch in diameter which extended across the jet. This holder gives the wedge type of flame pictured on page where the burning takes place on two flame surfaces. The third holder, a short piece of wire $1/32$ inch diameter, $1/2$ inch long was soldered to a fine wire and suspended across the jet; this holder forms a wedge type of flame surface where burning takes place on four surfaces.

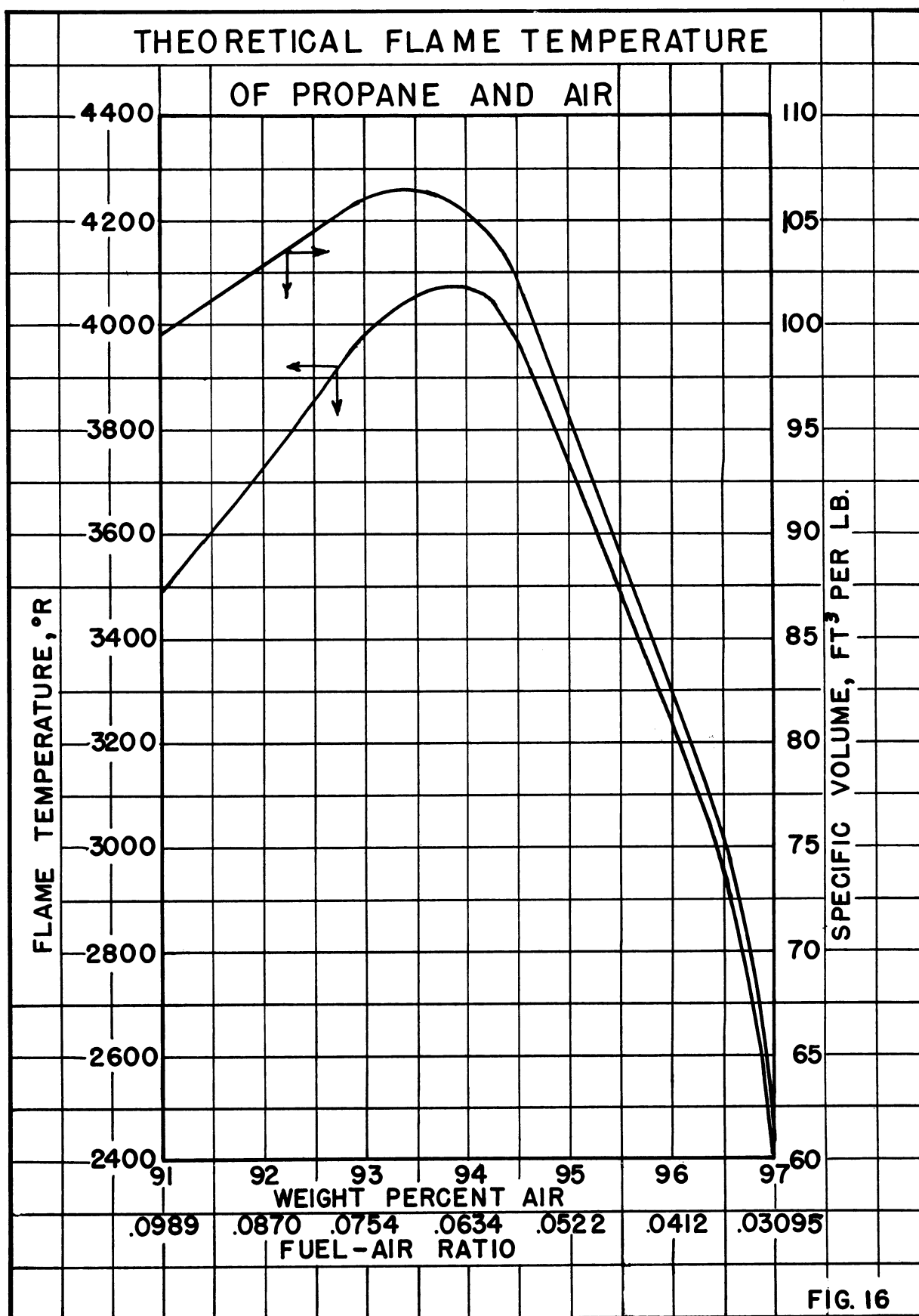


THE V- FLAME SYSTEM FOR
MEASURING FLAME SPEEDS

FIGURE 15

Flame speed as defined by equation (4) $V_f = \rho_b / \rho_u \sin \theta / 2 V_j$ requires the knowledge of three variables, ρ_b / ρ_u , θ , and V_j . The values of ρ_b were originally taken from a theoretical equilibrium analysis of propane and air mixtures, and ρ_u was computed from the conditions of the test. The theoretical values of $v = \frac{1}{\rho_b}$ as a function of F/A ratio are given in Figure 16, and the theoretical values of ρ_b / ρ_u are given in curve (B) Figure 17. These theoretical values were soon questioned and the steady flow

UMM-21



UMM-21

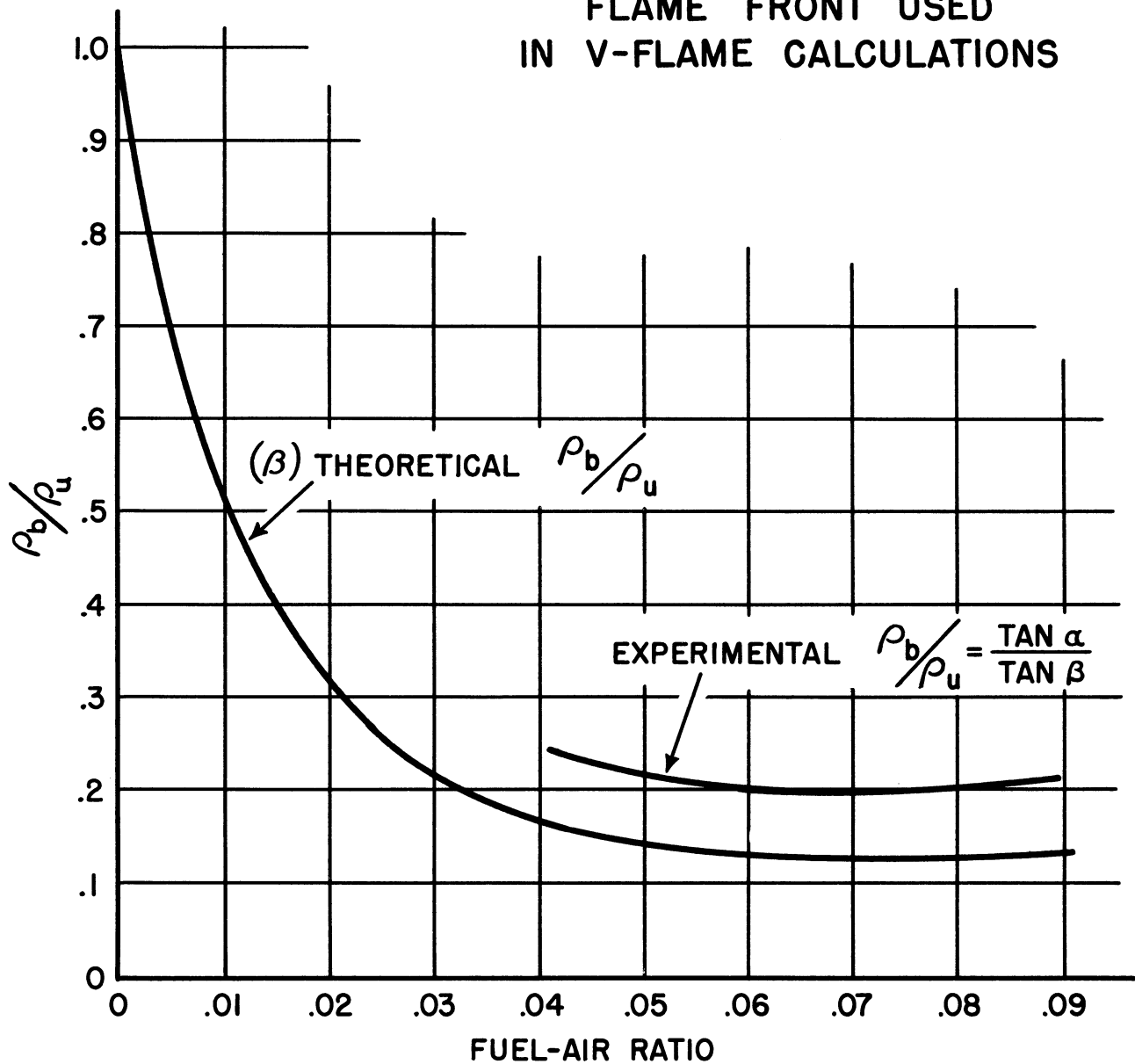
DENSITY RATIO ACROSS
FLAME FRONT USED
IN V-FLAME CALCULATIONS

FIG. 17

analysis of page 11 was derived yielding

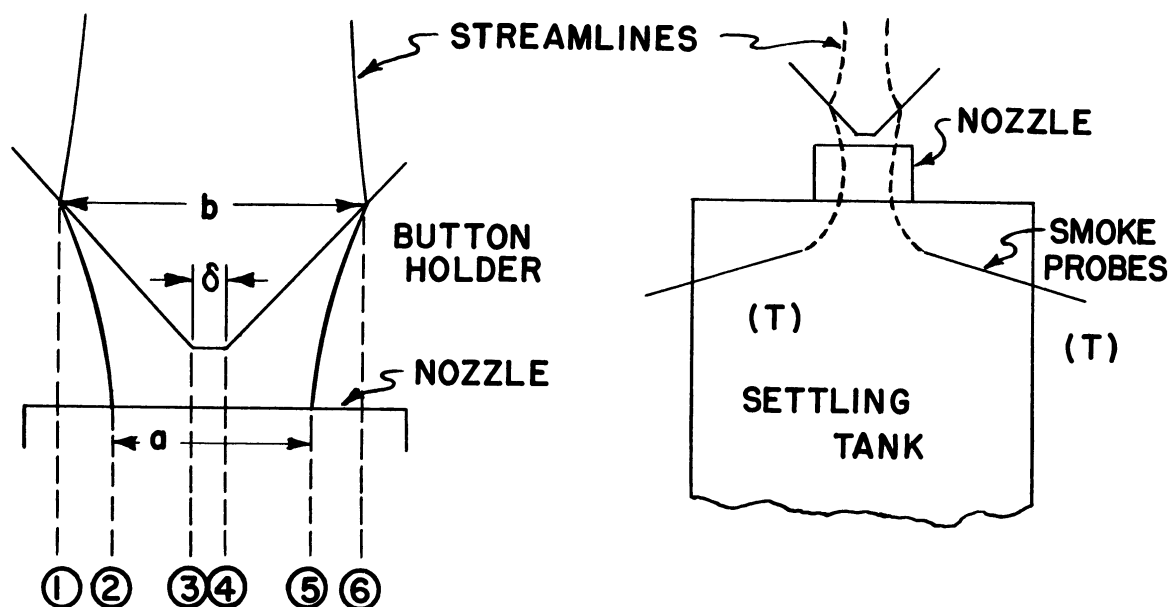
$$\rho_b / \rho_u = \frac{\tan \alpha}{\tan \beta} \quad (7b)$$

Since the angles α and β can be measured by the streamline method mentioned later in this report, it was possible to determine the experimental values of ρ_b / ρ_u . These experimental values and the theoretical values are quite different as shown in Figure 17. After this steady flow analysis was made, all additional flame speed computation of the V-Flame were made using the experimental values of ρ_b / ρ_u in equation 4.

The jet speed, V_j , was obtained by measuring the total head in the settling tank and then computing the jet velocity.

It was possible with the use of a goniometer mounted on a micrometer slide to measure the flame angle θ with a very high degree of accuracy. The goniometer consisted of a protractor which was marked off in $1/4$ degrees and mounted on a block through which a telescope extended. The cross hairs of the telescope then turned with the arm of the protractor. The goniometer and micrometer were mounted on a telescoping stand about three feet from the flame.

The V-flame area method for measuring flame speed, that is, $V_f = A_j V_j / A_f$ is seemingly a very simple method. Practical aspects, however, make this method very difficult to use, since it requires two distinct streamlines, A-A and B-B exist in the flow field, as shown in Figure 18. To obtain these streamlines, a very dense and luminous smoke produced by the mixture of vapors of titanium tetrachloride and the moisture in the air, was forced through the small glass tubes (T) located in the settling chamber, as shown in Figure 18. Due to the large contraction ratio of the jet, the smoke as it issued from the nozzle formed very fine streamlines. One of the most difficult problems of this method was obtaining and maintaining these streamlines. The titanium tetrachloride as it mixed with air not only forms smoke, but also forms titanium oxide and hydrochloric acid. When these latter products are mixed a sticky gum forms on the glass tubes. This gum soon clogs the smoke nozzles and necessitates cleaning the probes after each run, making the process slow and tedious.



STREAMLINES USED FOR V-FLAME AREA
METHOD OF MEASURING FLAME SPEED

FIGURE 18

By consideration of the conical flame, pictured in Figure 18,

$$V_f = V_j A_j / A_f = \frac{a^2}{b^2 - \delta^2} \times V_j \sin \theta / 2. \text{ After the streamlines were placed}$$

in position, the readings a , b , and δ were made with the micro-meter slide and θ was measured with the goniometer. V_j was measured in the same manner as it was for the V-flame angle method. (Page 28)

THE METHOD USED FOR TAKING SHADOWGRAPHS

The shadowgraph method of photography requires that light rays from a point source pass through a region of varying density and thence to a screen or photographic plate. Since the flame front is essentially a surface of density discontinuity, it can be photographed by this method. The main difficulty encountered is the fogging of the photographic plate which results from the intense radiation of the flame.

The shutter shown in Figure 19 was operated manually by pulling it up against the tension of the spring and then releasing it. As the shutter passed point (c) an electrical contact was made which discharged a condenser through the mercury arc lamp. Since the mercury arc lamp has a 5 microsecond flash, all motion in the flame was essentially stopped, and because of the fast action of the shutter the film was not fogged.

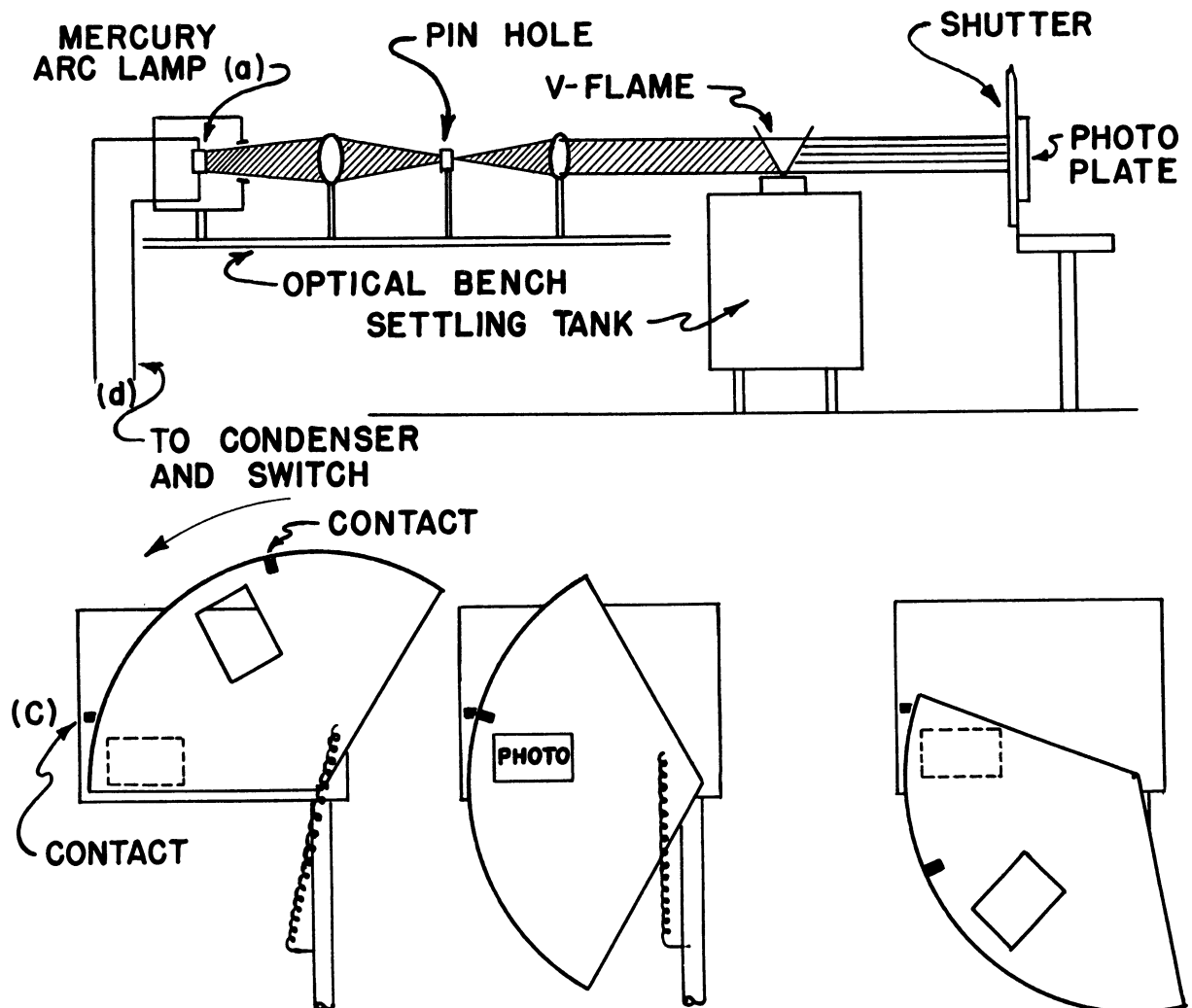


FIGURE 19

R E F E R E N C E S

Reference

No.

1. Gouy, Ann. Chim. Phys., 18, 27 (1879).
2. Stevens, F. W., NACA Reports 305(1929); 372 (1930).
3. Bunsen, R., Poggendorffs Ann., 131, 161 (1866).
4. Smith, F. A., and S.F. Pickering, J. Research
National Bureau of Standards, 17, 7 (1936).

LIST OF ILLUSTRATIONS

<u>Illustration</u>	<u>Title</u>	<u>Page</u>
1.	Conical V-Flame with Streamlines of TiCl_4	33
2.	Typical V-Flame in a Non-turbulent Air Stream	34
3.	Chalk Particles Describing Flow Field about V-Flame	35
4.	Pilot Flame in Wake of Flame Holder	36
5.	Shadowgraph of a V-Flame in a Laminar Gas Stream	37
6.	Shadowgraph of a V-Flame in a Turbulent Gas Stream	37
7.	Shadowgraph of Laminar Flow Past a Heated Flame Holder	38
8.	Shadowgraph of Turbulent Flow Past a Heated Flame Holder	38
9.	Typical V-Flame in a Turbulent Air Stream	39

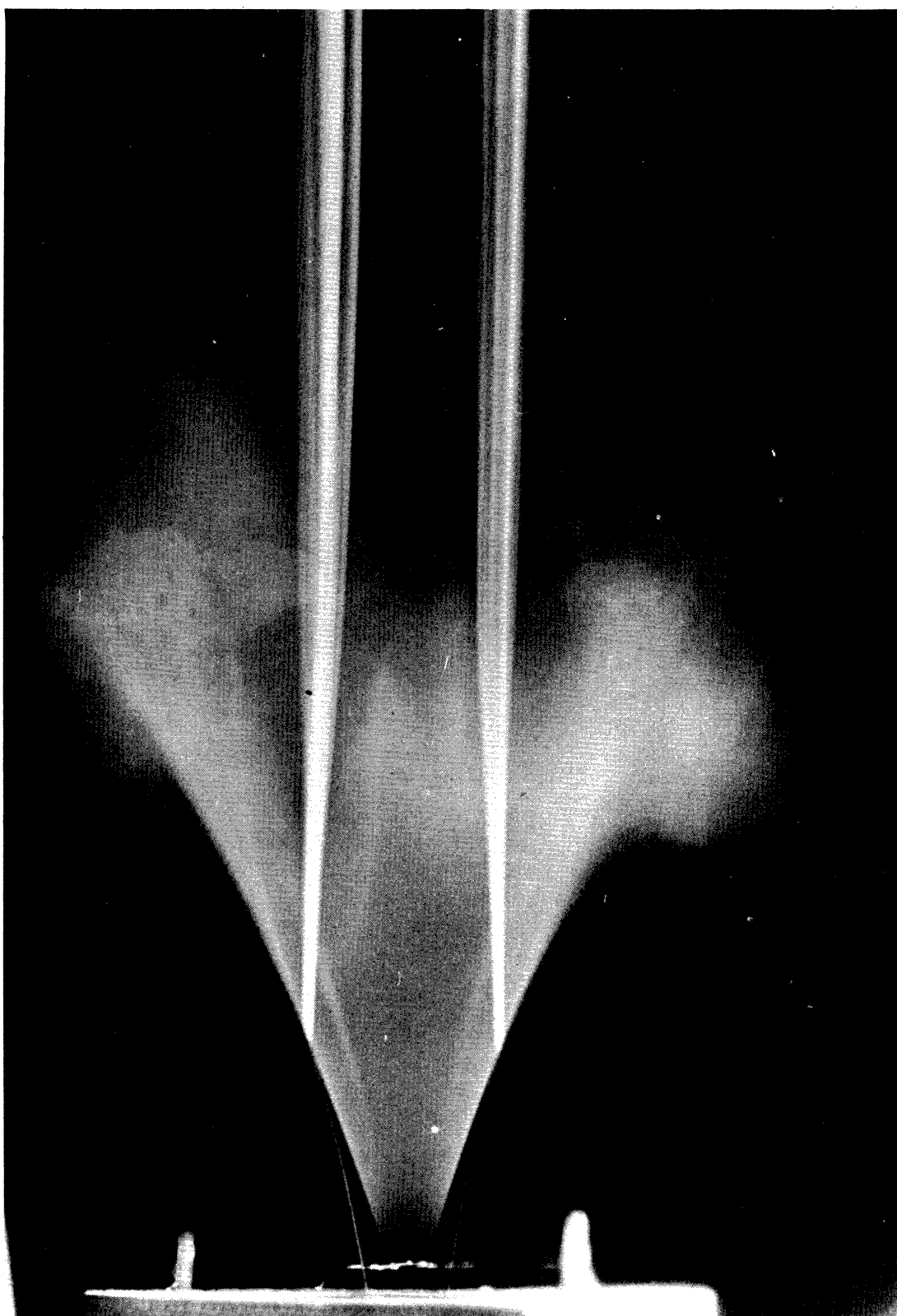
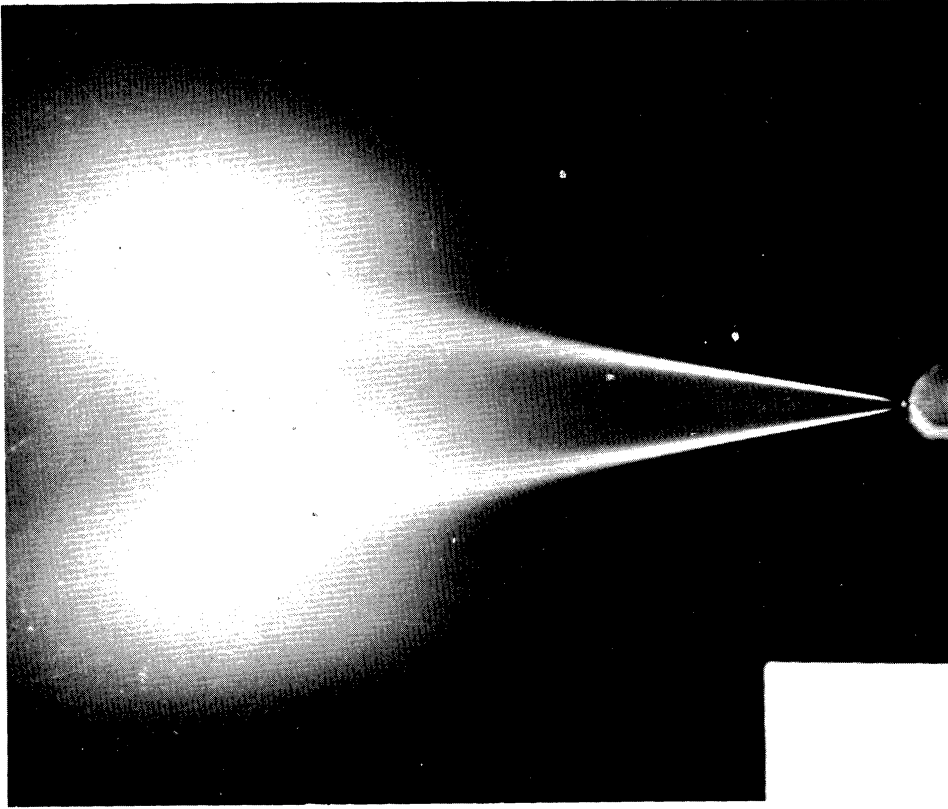
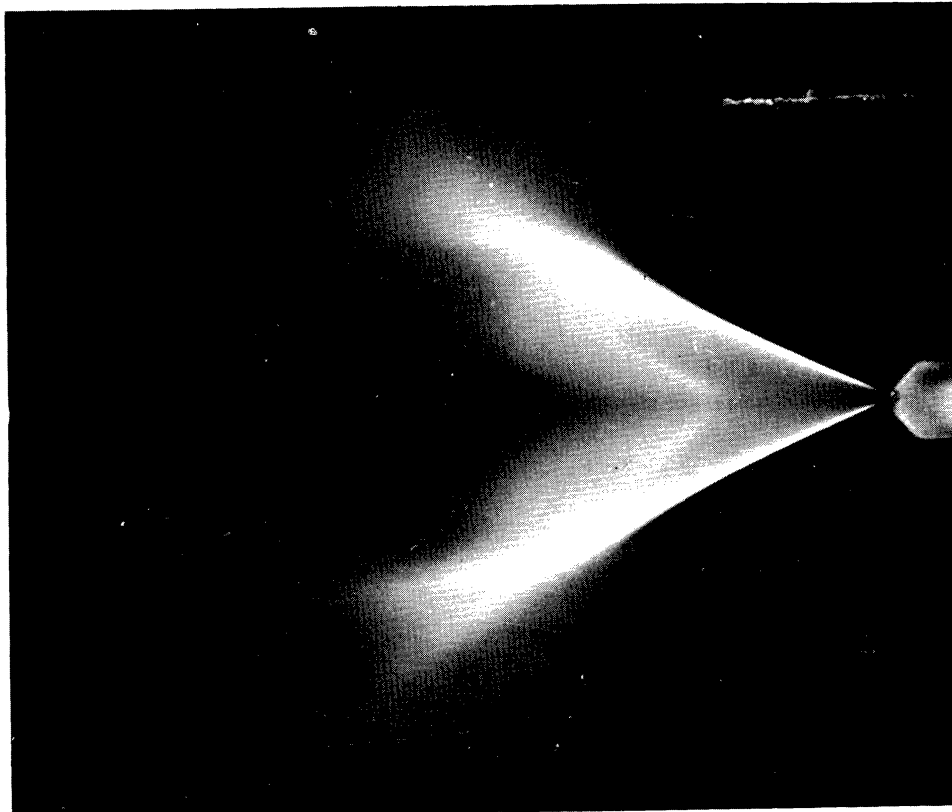


ILLUSTRATION 1 - CONICAL V-FLAME WITH STREAMLINES of TiCl_4

UMM-21



$V_j = 32.2 \text{ ft/sec}$ $F/A = .0798$



$V_j = 15.3 \text{ ft/sec}$ $F/A = .0543$

ILLUSTRATION 2 - TYPICAL V-FLAME IN A NON-TURBULENT
STREAM

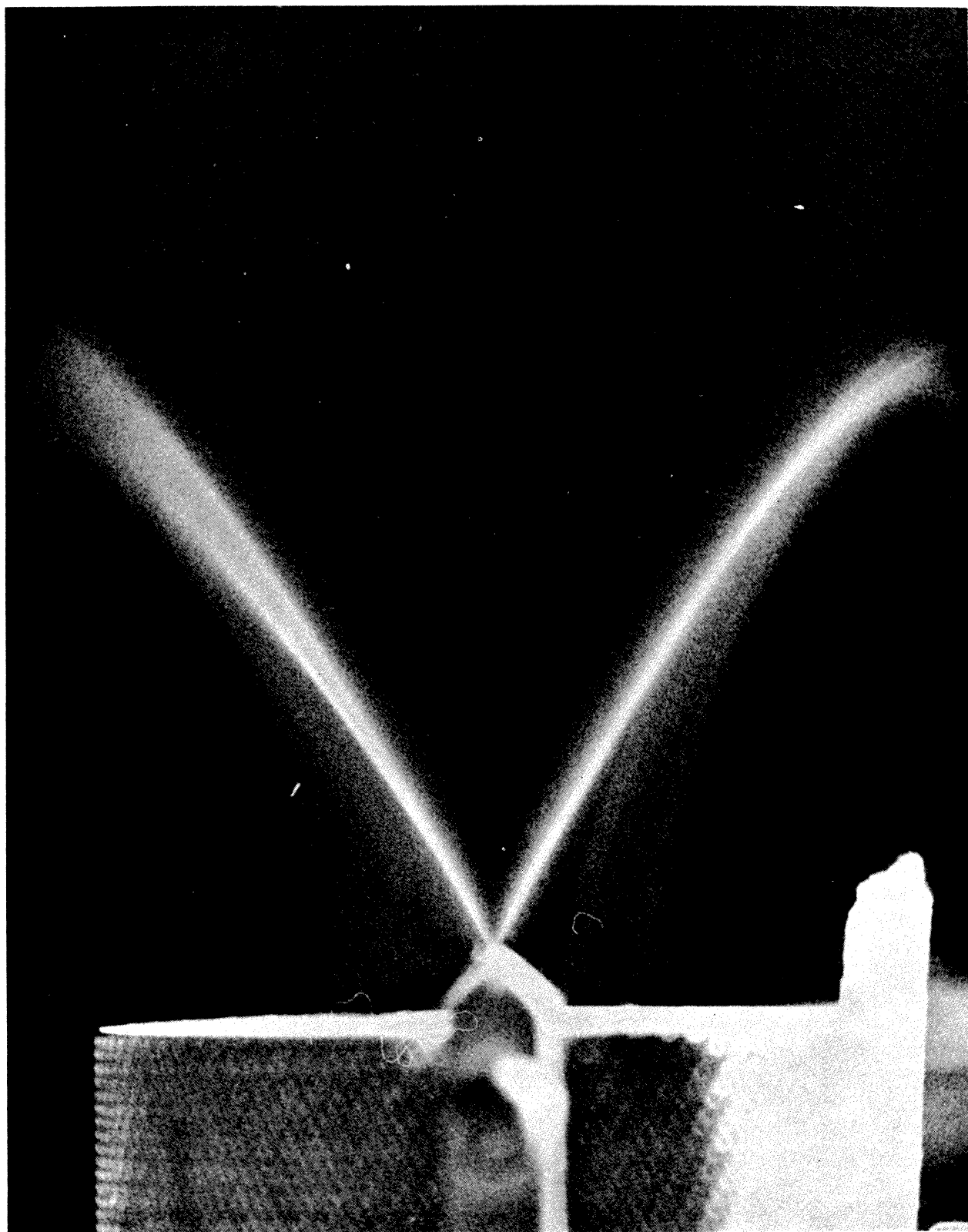


ILLUSTRATION 3 - CHALK PARTICLES DESCRIBING FLOW FIELD ABOUT
V-FLAME

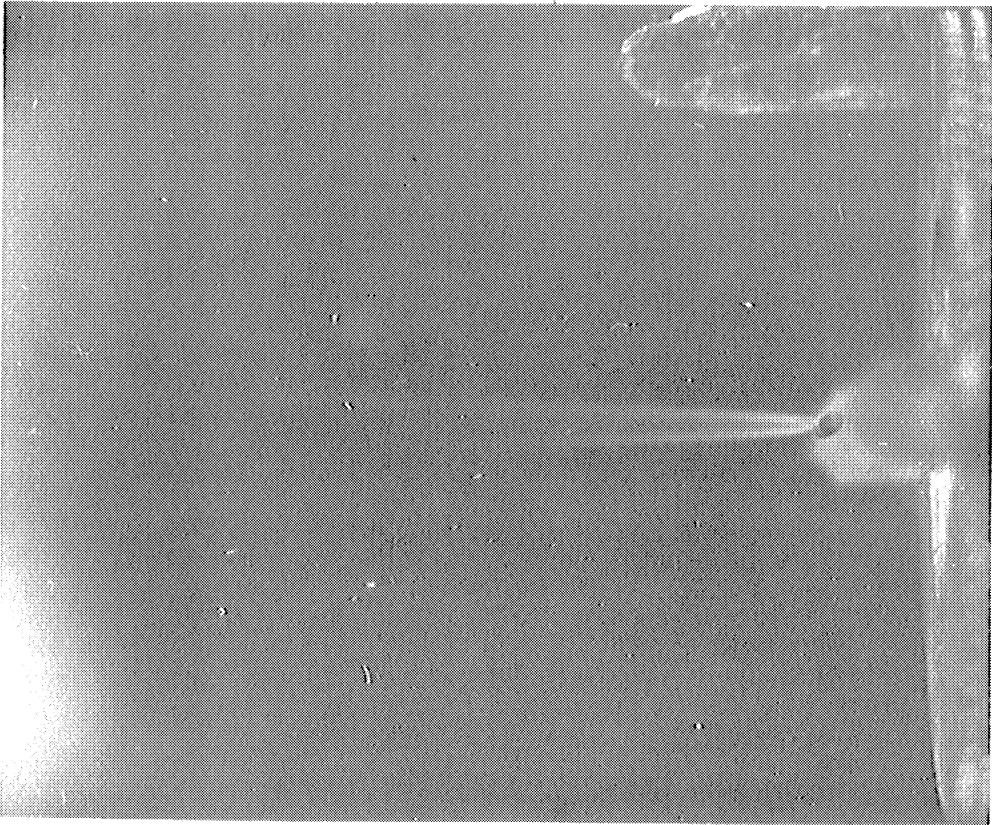
UMM-21



BUTTON FLAME HOLDER

d .15 in

ILLUSTRATION 4 - PILOT FLAME IN WAKE OF FLAME HOLDER. THE MAIN BULK OF THE COMBUSTIBLE GASES EITHER BURN ABOVE THE PILOT FLAME OR DO NOT BURN AT ALL.



ROD FLAME HOLDER

d .04 in

UMM-21

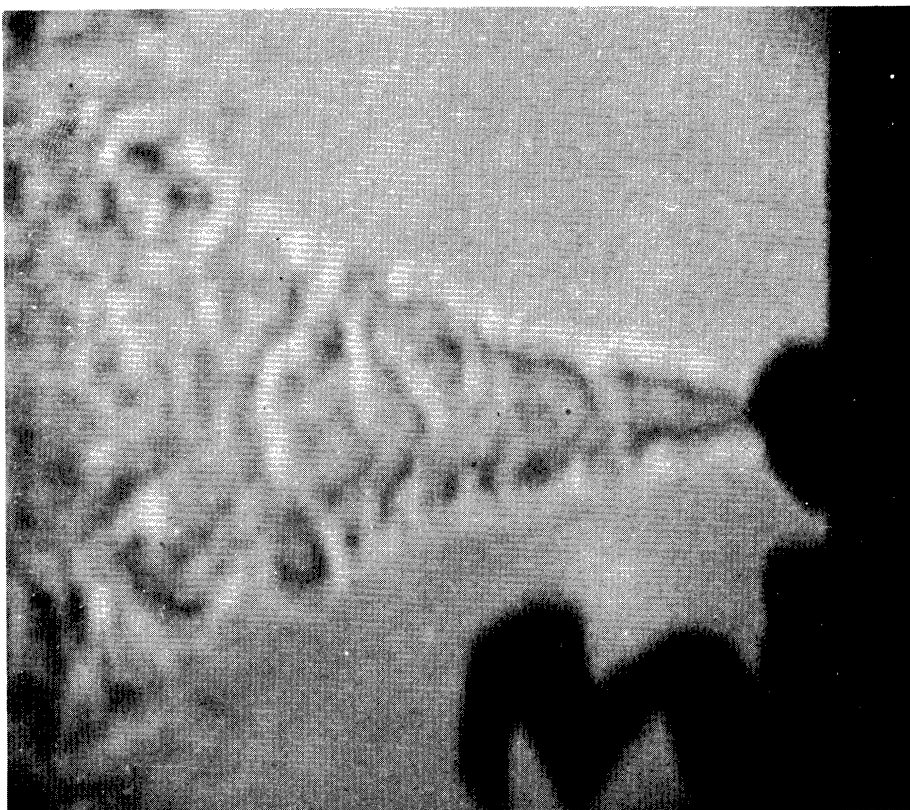


ILLUSTRATION 6 - SHADOWGRAPH OF A
V-FLAME IN A TURBULENT GAS STREAM

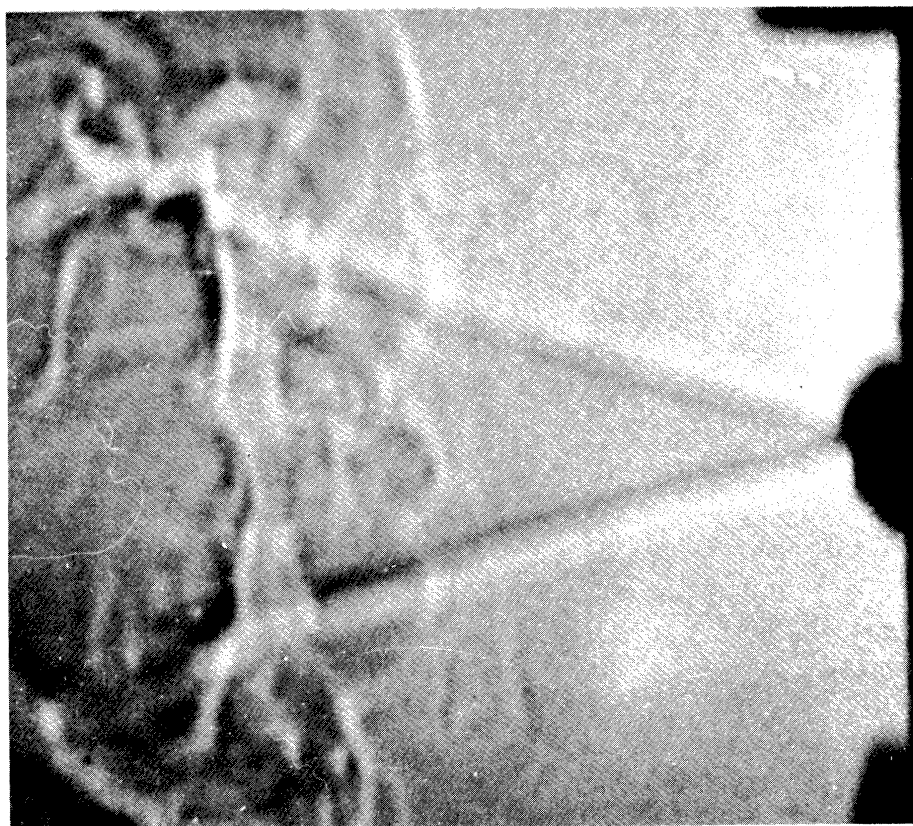


ILLUSTRATION 5 - SHADOWGRAPH OF A
V-FLAME IN A LAMINAR GAS STREAM

UMM-21

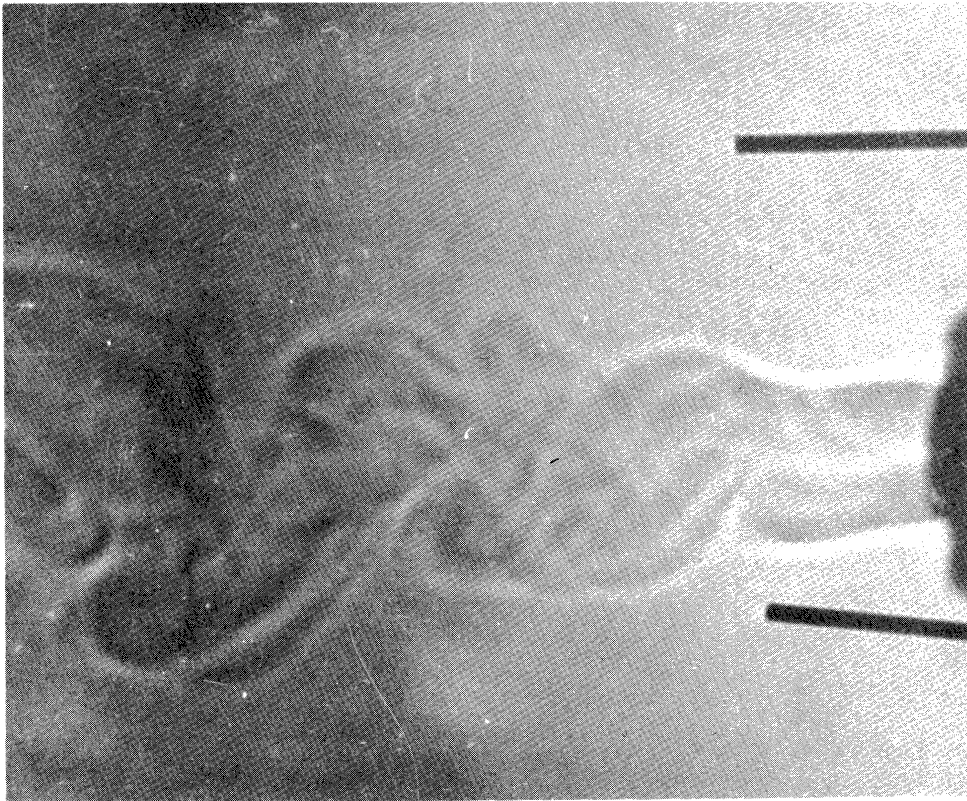


ILLUSTRATION 7 - SHADOWGRAPH OF A
FLOW PAST A HEATED FLAME HOLDER

LAMINAR AIR STREAM

$V_j = 14.8 \text{ ft/sec}$

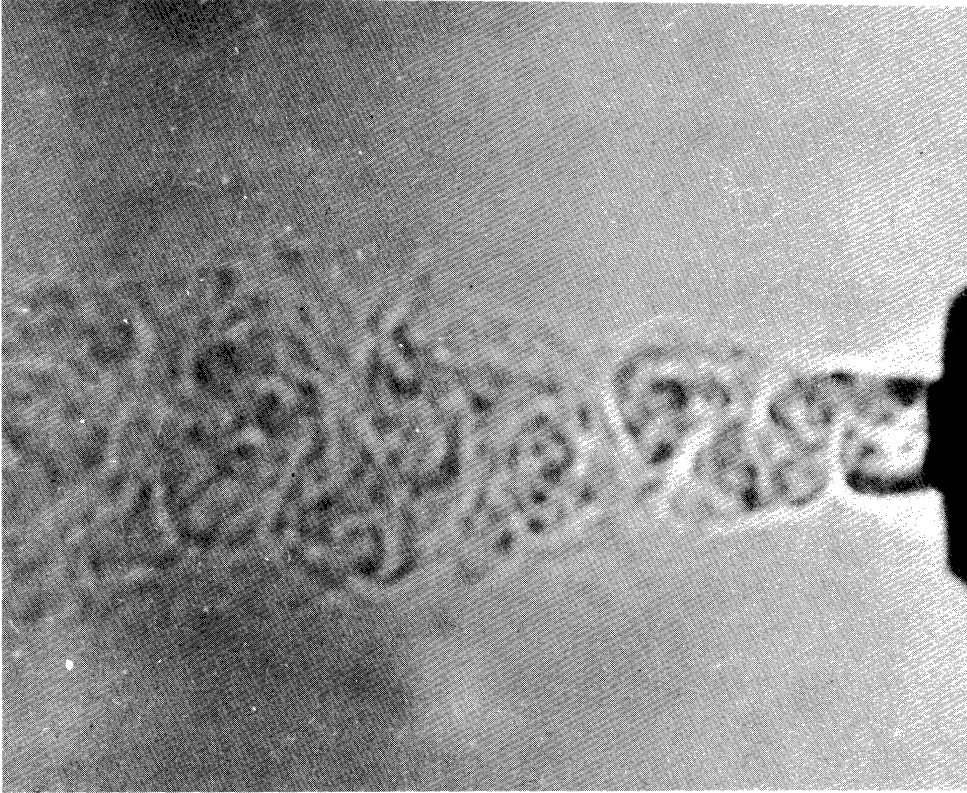


ILLUSTRATION 8 - SHADOWGRAPH OF
TURBULENT FLOW PAST A HEATED
FLAME HOLDER

TURBULENT AIR STREAM

$V_j = 14.8 \text{ ft/sec}$

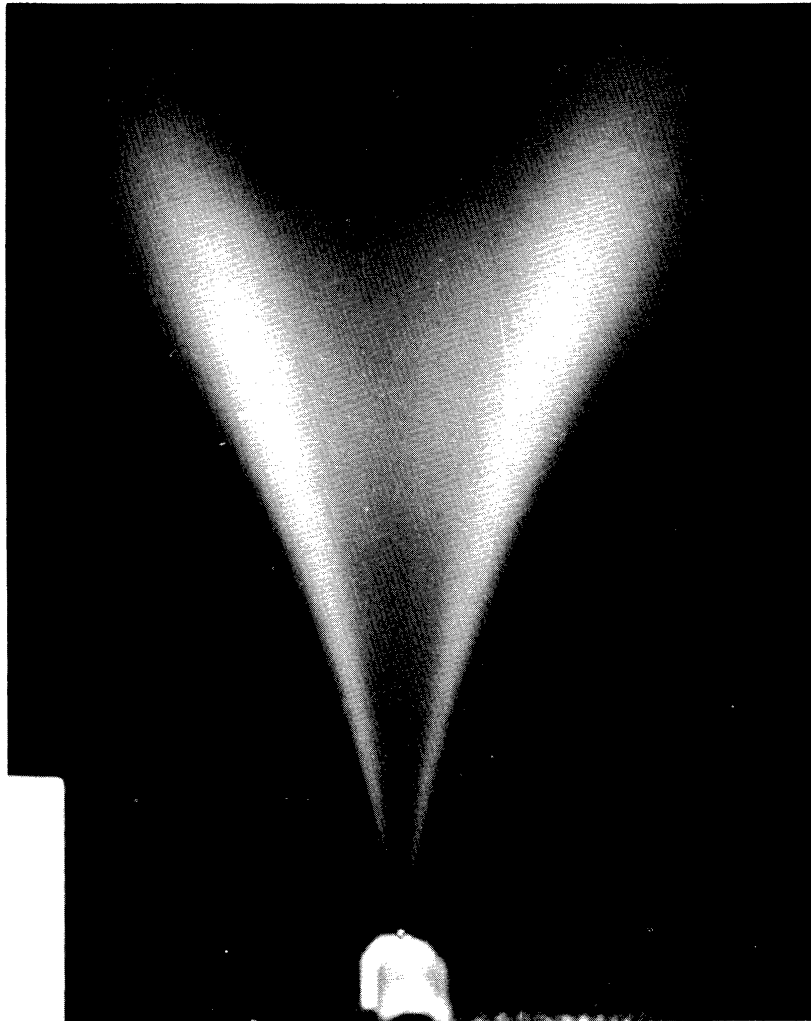


ILLUSTRATION 9 - TYPICAL V-FLAME IN A TURBULENT AIRSTREAM

$$V_j = 34 \text{ ft/sec} \quad F/A = .0634$$

DISTRIBUTION

Distribution of this report is made in
accordance with ANAF-G/M Mailing List
No. 8, dated 1 April 1949, to include
Part A, Part B and Part C.

UNIVERSITY OF MICHIGAN



3 9015 03483 1605